

## RADIAL VELOCITIES FOR 889 LATE-TYPE STARS<sup>1</sup>

DAVID L. NIDEVER,<sup>2</sup> GEOFFREY W. MARCY,<sup>2,3</sup> R. PAUL BUTLER,<sup>4</sup> DEBRA A. FISCHER,<sup>3</sup> AND STEVEN S. VOGT<sup>5</sup>

Received 2001 November 29; accepted 2002 March 10

### ABSTRACT

We report radial velocities for 844 FGKM-type main-sequence and subgiant stars and 45 K giants, most of which had either low-precision velocity measurements or none at all. These velocities differ from the standard stars of Udry et al. by  $0.035 \text{ km s}^{-1}$  (rms) for the 26 FGK standard stars in common. The zero point of our velocities differs from that of Udry et al.:  $\langle V_{\text{Present}} - V_{\text{Udry}} \rangle = +0.053 \text{ km s}^{-1}$ . Thus, these new velocities agree with the best known standard stars both in precision and zero point, to well within  $0.1 \text{ km s}^{-1}$ .

Nonetheless, both these velocities and the standards suffer from three sources of systematic error, namely, convective blueshift, gravitational redshift, and spectral type mismatch of the reference spectrum. These systematic errors are here forced to be zero for G2 V stars by using the Sun as reference, with Vesta and day sky as proxies. But for spectral types departing from solar, the systematic errors reach  $0.3 \text{ km s}^{-1}$  in the F and K stars and  $0.4 \text{ km s}^{-1}$  in M dwarfs.

Multiple spectra were obtained for all 889 stars during 4 years, and 782 of them exhibit velocity scatter less than  $0.1 \text{ km s}^{-1}$ . These stars may serve as radial velocity standards if they remain constant in velocity. We found 11 new spectroscopic binaries and report orbital parameters for them.

*Subject headings:* binaries: spectroscopic — catalogs — stars: fundamental parameters — stars: kinematics — stars: late-type — techniques: radial velocities — techniques: spectroscopic

*On-line material:* machine-readable tables

### 1. INTRODUCTION

The radial velocity of a star is ideally the component of the velocity vector of its center of mass that lies along the line of sight. Radial velocities are valuable for a variety of astrophysical investigations, including studies of the structure of the Milky Way Galaxy, the orbits of long-period binary stars, and the distances to star clusters (see, e.g., Binney & Merrifield 1998). “Barycentric” radial velocities (sometimes referred to as “absolute” radial velocities), such as reported here, are measured relative to the barycenter, or center of mass, of the solar system. Such velocities are often (incorrectly) termed “heliocentric,” though the Sun moves with a speed of  $\sim 13 \text{ m s}^{-1}$  relative to the barycenter.

Radial velocities of stars in the Galaxy are often measured with an accuracy of only  $\sim 0.5 \text{ km s}^{-1}$ . With advances in the accuracy of proper motion measurements to  $\sim 1 \text{ mas yr}^{-1}$  (e.g., Perryman et al. 1996) for many stars, a corresponding increase in the accuracy of radial velocities is required. Meanwhile, the best *relative* radial velocities have precisions of  $3 \text{ m s}^{-1}$  (Butler et al. 2000) and new instruments (e.g., HARPS) are designed to achieve a precision of  $1 \text{ m s}^{-1}$  (Bouchy et al. 2001; Pepe et al. 2000). These relative velocities have proved useful in the detection of extrasolar

planets (e.g., Marcy, Cochran, & Mayor 2000) but they are not necessarily tied to a velocity zero point. Nonetheless, the precision-velocity instruments have overcome many observational and technical hurdles related to spectroscopic Doppler-shift measurements, either by using a gas absorption cell or a fiber-fed comparison lamp spectrum (Valenti, Butler, & Marcy 1995; Butler et al. 1996; Baranne 1999).

The precision-velocity technology has been applied to the establishment of barycentric radial velocities, most notably by the Geneva team (Udry, Mayor, & Queloz 1999a; Udry et al. 1999b). They have measured velocities for 38 stable dwarf stars with precision better than  $0.05 \text{ km s}^{-1}$ .

Here we provide barycentric radial velocities with typical accuracies of  $0.3 \text{ km s}^{-1}$  (and precise to  $0.03 \text{ km s}^{-1}$  for a given spectral type) for 889 stars. Our intent is to provide a velocity measurement at the current epoch for a variety of purposes. Velocity variations with a timescale of hundreds of years may be detected by comparison of present and future velocities. We also hope to establish radial velocity standard stars, by identifying a subset that exhibit no significant velocity variation above  $10 \text{ m s}^{-1}$ .

### 2. BARYCENTRIC RADIAL VELOCITIES

The Doppler searches for planets have been successful because of the relative ease with which the change in radial velocity may be measured with high internal precision. Such relative velocities circumvent the technical challenges associated with the determination of an accurate velocity zero point, and they avoid the physical interpretation of a barycentric Doppler shift which becomes bewildering at levels below  $1 \text{ km s}^{-1}$ .

Barycentric Doppler shifts carry an unclear interpretation for several reasons. Stellar lines suffer a gravitational redshift (Misner, Thorne, & Wheeler 1973) upon leaving the

<sup>1</sup> Based on observations obtained at the W. M. Keck Observatory, which is operated jointly by the University of California and the California Institute of Technology, and on observations obtained at the Lick Observatory, which is operated by the University of California.

<sup>2</sup> Department of Physics and Astronomy, San Francisco State University, San Francisco, CA 94132; dnidever@stars.sfsu.edu.

<sup>3</sup> Department of Astronomy, University of California, Berkeley, CA 94720.

<sup>4</sup> Department of Terrestrial Magnetism, Carnegie Institution of Washington, 5241 Broad Branch Road NW, Washington, DC 20015-1305.

<sup>5</sup> UCO/Lick Observatory, University of California at Santa Cruz, Santa Cruz, CA 95064.

stellar photosphere, yielding effective redshifts of  $V_{\text{grav}} = GM/Rc$  (Dravins et al. 1999). This redshift varies from  $680 \text{ m s}^{-1}$  for F5 V to  $500 \text{ m s}^{-1}$  for M5 V stars, the range of spectral types considered here. Uncertainties in stellar masses and radii prevent an accurate removal of this effect. Furthermore, stellar lines suffer a transverse Doppler effect (essentially time dilation), the removal of which requires knowledge of the full velocity vector of the star's space motion. This effect is  $\simeq 50 \text{ m s}^{-1}$  for the fastest moving stars (Lindegren, Dravins, & Madsen 1999).

More importantly, stellar Doppler shifts are affected by subphotospheric convection (granulation), macroturbulence, stellar rotation, pressure shifts, oscillations, and activity cycles. The most important of these effects is granulation. The textbook explanation is that a larger contribution to the stellar flux emerges from hot, rising gas than from falling gas in the convective cells. These motions yield an overall blueshift of spectral lines (Dravins 1999). However, the exact convective blueshift depends on the full three-dimensional hydrodynamics and radiative transfer in each spectral line as a function of depth in the photosphere (Dravins 1999). The blueshift clearly depends on spectral type and is expected to be  $\sim -1000 \text{ m s}^{-1}$  for F5 V,  $-400 \text{ m s}^{-1}$  for G2 V, and  $-200 \text{ m s}^{-1}$  for K0 V (Dravins et al. 1999). Effects due to pressure shifts are less than  $100 \text{ m s}^{-1}$  for ordinary stars (Dravins et al. 1999; Allende Prieto et al. 1997). Stellar rotation also imposes minor radial velocity effects (Gray 1999).

Moreover, the measurement of spectroscopic barycentric radial velocities usually requires a reference stellar spectrum. Due to constraints of telescope time and available standard stars, only a small number of reference spectra can be used. Typically, the Doppler measurements require use of reference spectra having different spectral types than the program star, which leads to spectral mismatch errors. Since the strengths of spectral lines vary with temperature and metallicity, the spectra of the reference and program stars will be significantly different. In effect, the relative displacement in wavelength between two nonidentical spectra is not uniquely defined and therefore is dependent on the algorithm used. Such spurious Doppler effects are minimized, but not eliminated, by using high-resolution spectra with many lines resolved, as adopted in this present survey.

The effects of convection, stellar gravitational redshift, transverse Doppler shift, and the other effects mentioned above cannot be determined for a star with an accuracy that is comparable to the internal measurement errors of  $\sim 10 \text{ m s}^{-1}$ . Removal of such effects by a model of each star might introduce more model-dependent errors. Nonetheless, with considerable modeling, the measurement of a Doppler shift may be used to determine the "true" velocity component of the center of mass of the star. Alternatively (and more traditionally), Doppler measurements may be left merely as an observable, namely the spectroscopic shift in wavelength, often quoted as  $z = \Delta\lambda/\lambda_0$  (Lindegren et al. 1999).

Here we adopt the philosophy that spectroscopic barycentric radial velocities should first be corrected for local effects, such as that caused by the observer's motion relative to the solar system barycenter ( $\sim 30 \text{ km s}^{-1}$ ) and by the solar gravitational blueshift ( $\sim 3 \text{ m s}^{-1}$ ). In addition, we will correct all of our velocities of FGK stars for gravitational redshift and convective blueshift to first order by using the known radial velocity of the Sun to set the zero point for the stellar velocity measurements.

Our quoted Doppler shifts represent velocities as if measured at the solar system barycenter but with the Sun and its potential well removed. Clearly, the velocity measurements presented here are amenable to future corrections for the spectral-type dependence relative to G2 V for gravitational redshift and convective blueshift, in order to yield the most accurate velocities possible for them (e.g., Gullberg 1999; Saar & Fischer 2000).

### 3. SPECTROSCOPIC OBSERVATIONS

The spectra were obtained with the HIRES echelle spectrometer (Vogt et al. 1994) on the 10 m Keck I telescope and with the "Hamilton" echelle spectrometer fed by either the 3 m Shane or the 0.6 m Coude Auxilliary (CAT) Telescopes (Vogt 1987). During an observation the starlight is sent through a glass cell that is filled with iodine vapor (Marcy & Butler 1992) before entering the spectrometer, which superimposes iodine lines on the stellar lines. These iodine absorption lines are used to calibrate the wavelength scale of the spectrum from 5000 to 6000 Å.

Our Doppler planet search project contains 889 stars at the Keck and Lick Observatories (Butler et al. 2000). Until now only relative radial velocities have been computed from these spectra, and they have a precision of  $\sim 3 \text{ m s}^{-1}$  (Butler et al. 1996; Vogt et al. 2000), which has allowed the discovery of Jovian and sub-Jovian sized extrasolar planets (Marcy et al. 2000).

To achieve barycentric velocities, we adopt two standard spectra. We use the National Solar Observatory (NSO) FTS solar spectrum (Kurucz et al. 1984) and an M dwarf composite spectrum (see § 4) as reference spectra. The 889 stars each typically have  $\sim 12$  spectra obtained during 4 years from 1997 to 2001. The distribution of spectral types in our sample is: 14% F, 46% G, 27% K, and 13% M stars. Except for 45 K giants all stars are main-sequence dwarfs or subgiants. All stars are void of a visible companion within  $2''$ , though some were subsequently revealed to be spectroscopic binaries (see § 9).

### 4. DOPPLER METHOD

The barycentric radial velocities reported here are found in a manner similar to that used to find the relative radial velocities for the planet search. An observed spectrum is fitted with a synthetic spectrum that is composed of the individual stellar and iodine spectra. In detail, the synthetic spectrum is the product of the deconvolved stellar "template" spectrum (with the spectrometer instrumental profile removed) with a high-resolution spectrum of molecular iodine. The product of these two is convolved with the instrumental profile of the spectrometer (at the time of the observation), to produce the final synthetic spectrum, as described in Butler et al. (2000).

The observed spectrum to be synthesized is broken into "chunks" of length 40 pixels corresponding to roughly  $\sim 2 \text{ Å}$ . In total 14 free parameters are fitted in the Doppler analysis; 11 devoted to the instrumental profile, along with the wavelength zero point of each chunk, the wavelength dispersion across each chunk, and the Doppler shift of the stellar spectrum relative to the stellar template of that star,  $z$  ( $=\Delta\lambda/\lambda$ ). All of the parameters, except for  $z$ , are extracted primarily from the iodine portion of the observed spectrum. After the best parameters are found for all the chunks of a

spectrum they are saved for further analysis, notably the weighted average of  $z$ . We apply a correction to all velocities for our topocentric motion relative to the barycenter (McCarthy 1995). For a more in-depth discussion of this standard Doppler analysis to obtain relative velocities, see Marcy & Butler (1992), Butler et al. (1996), and Valenti et al. (1995).

To obtain barycentric radial velocities, the approach was similar to the standard analysis described above and indeed we used some parameters derived from that analysis. Here we used the National Solar Observatory (NSO) solar spectrum (Kurucz et al. 1984) as the deconvolved template, for all F, G, and K stars. For M dwarfs, we constructed an in-house M star composite spectrum as the template (see below). Since all parameters except for  $z$  are extracted from the iodine portion of the spectrum previously, the use of a different stellar template spectrum does not affect these parameters significantly. Therefore, in our new fit, we simply adopt the values of the 13 non- $z$  parameters that were previously obtained in the Doppler analysis for relative velocities (i.e., for the planet search) and we fit here only for the barycentric radial velocity,  $z$ .

Ordinarily, when the deconvolved stellar spectrum of the individual star is used as the template, the  $\chi^2_\nu$  statistic is near unity (usually less than 1.7), because the stellar contribution to the model is a previously obtained deconvolved spectrum of the same star. But in our fit for barycentric velocities, the value of reduced  $\chi^2_\nu$  is much larger (poorer) because of the mismatch between the template spectrum (NSO or M dwarf composite) and that of the program star. The program star differs from the solar or M-dwarf template in spectral type, metallicity, and  $v \sin i$ . Thus, the spectral fits are not as good, yielding  $\chi^2_\nu$  of 3–7.

The internal error per observation, as defined by the weighted standard deviation of the mean of the velocities from all ( $\sim 400$ ) chunks, is higher for our barycentric radial velocities than for the relative radial velocities used in the planet search. We find that while the relative velocities carry errors of  $\sim 3 \text{ m s}^{-1}$  (for the planet search) the average internal error per observation for the barycentric velocities reported here is  $\sim 20 \text{ m s}^{-1}$ . A more conservative estimate of our velocity precision is given in § 6 as  $0.03 \text{ km s}^{-1}$  from comparison with the standard stars.

Due to the fact that only one stellar template is used for a large range of stellar types, we expect that our errors (internal error per observation) will depend on  $B-V$ . The greater the difference between template and program star, the greater the expected error due to spectral mismatch. We plot this internal error in our barycentric velocities versus  $B-V$  in Figure 1. Since the NSO solar spectrum,  $B-V = 0.64$  (Carroll & Ostlie 1996), is used for F, G, and K stars we expect the errors to be minimized for solar type stars. This is confirmed in Figure 1. The M dwarf composite template spectrum was created from five different M dwarfs having average spectral type of M3 (see below). The internal velocity errors for stars analyzed with this stellar template are minimized at  $B-V \approx 1.5$ , as can also be seen in Figure 1.

Each program star has an average of 12 observations. As many observations as possible are analyzed per star, up to 30, in order to minimize the uncertainty in the mean of the barycentric radial velocities. If the radial velocity of the star were stable we should obtain an uncertainty in the mean of  $\sim 20/\sqrt{12} \approx 6 \text{ m s}^{-1}$ . A majority of stars indeed exhibit velocity scatter of  $\sim 10 \text{ m s}^{-1}$  (rms), while others have an rms

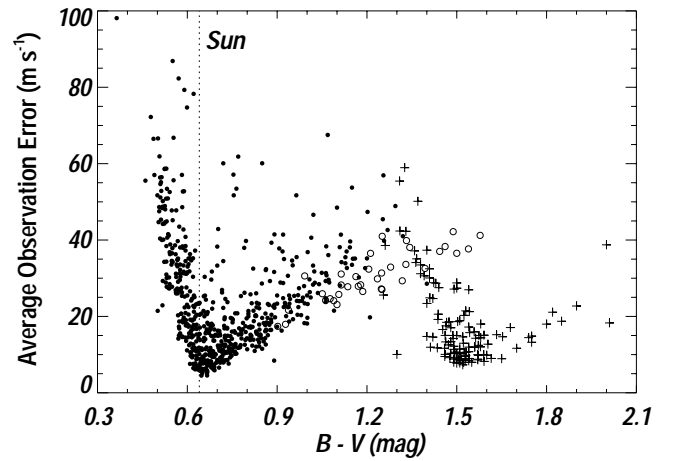


FIG. 1.—Internal velocity error per observation (averaged per star) vs.  $B-V$ . The dots represent the stars for which the NSO solar spectrum was used as the reference (filled dots represent dwarfs and open dots represent giants), and the pluses represent the stars for which the M star composite spectrum was used as the reference. The  $B-V$  for the Sun ( $B-V = 0.64$ ) is shown for clarity. The spectral type dependence of errors is apparent.

scatter larger than  $100 \text{ m s}^{-1}$ . Scatter in the latter stars is almost always caused by companions or large chromospheric activity. Overall, 782 of the 889 stars have an rms velocity scatter less than  $0.1 \text{ km s}^{-1}$ , and 107 stars have an rms velocity scatter larger than  $0.1 \text{ km s}^{-1}$ . The barycentric radial velocities for these stars are reported in Tables 1 and 2, respectively.

As mentioned above, the NSO solar spectrum could not be used as the template for the M dwarf program stars because the spectra are too different. Therefore, a separate reference spectrum was required for the M stars. For this purpose a composite spectrum of five M stars was produced in the following manner.

Five M stars were selected having barycentric radial velocities reported by Marcy, Lindsay, & Wilson (1987) with low uncertainties: GJ 251 (M4), GJ 411 (M2), GJ 526 (M4), GJ 752A (M3.5), and GJ 908 (M2). One spectrum of high S/N ratio was used from each of these M dwarfs. The spectra were shifted back, to remove the Doppler shifts caused by the barycentric motion of the observatory and by the barycentric radial velocity of the star itself relative to the barycenter, taken from Marcy et al. (1987). To check for any residual Doppler shifts, these corrected spectra were then cross-correlated with respect to one of them, GJ 251. Assuming the resulting displacements were due to random errors, the mean of the residual velocities was taken to be the barycentric velocity zero point. Using this reference point the spectra were again corrected for their Doppler shifts. Finally, the spectra were put on the same wavelength scale and co-added to create a M star composite spectrum.

## 5. VELOCITY ZERO POINT

Using observations of the day sky and the minor planet Vesta we found the zero point of our velocities for FGK stars. These references were used because they have essentially solar spectra, and the radial velocities of Vesta and the Sun relative to a topocentric observer are easily determined. We used the on-line “JPL Ephemeris Generator” to find

TABLE 1  
RADIAL VELOCITIES OF STABLE STARS<sup>a</sup>

Primary Name (1)	Alternate Name (2)	Ref. (NSO/M) (3)	(JD) (-2440000) (4)	$\Delta T$ (days) (5)	(RV) (m s <sup>-1</sup> ) (6)
HD 166	HIP 544	NSO	8783	2662	-6537
HD 283	HIP 616	NSO	11002	1185	-43102
HD 377	HIP 682	NSO	11417	208	1184
HD 400	HIP 699	NSO	11137	507	-15141
HD 531	BD +07 9	NSO	11419	208	13460
HD 1326A	GJ 15A	M	9928	4656	11814
HD 1326B	GJ 15B	M	11294	509	10976
HD 1388	HIP 1444	NSO	11016	1338	28498
HD 1461	HIP 1499	NSO	11083	1184	-10166
HD 1832	HIP 1813	NSO	11250	950	-30550
HD 1835	HIP 1803	NSO	9123	3026	-2405
HD 2025	HIP 1936	NSO	11218	1389	3241
HD 2774	HIP 2497	NSO	11478	117	-51566
HD 3074	HIP 2663	NSO	10955	1390	29539
HD 3079	HIP 2712	NSO	11193	390	-12347
HD 3651	HIP 3093	NSO	9708	4708	-32961
HD 3674	HIP 3119	NSO	11161	514	166
HD 3765	HIP 3206	NSO	11151	1294	-63202
HD 3861	HIP 3236	NSO	11055	105	-14796
HD 4203	HIP 3502	NSO	12020	431	-14140
HD 4208	HIP 3479	NSO	11345	1427	56726
HD 4256	HIP 3535	NSO	11069	1177	9460
HD 4307	HIP 3559	NSO	11303	1390	-10349
HD 4614	HIP 3821	NSO	9380	4080	8314
HD 4614B	GJ 34B	M	10036	1860	11293
HD 4628	HIP 3765	NSO	9262	3747	-10230
HD 4915	HIP 3979	NSO	11348	291	-3742
HD 5065	HIP 4127	NSO	11336	510	-73844
HD 5133	HIP 4148	NSO	11470	96	-13067
HD 5372	HIP 4393	NSO	11325	950	596
HD 6101	HIP 4849	NSO	11041	58	22170
HD 6611	HIP 5276	NSO	11027	0	-6068
HD 6734	HIP 5315	NSO	11130	1426	-94511
HD 7047	HIP 5534	NSO	11128	418	9264
HD 7228	HIP 5682	NSO	11450	509	-20538
HD 7590	HIP 5944	NSO	11425	27	-13073
HD 7727	HIP 5985	NSO	11262	514	5898
HD 8262	HIP 6405	NSO	11290	507	5636
HD 8389	HIP 6456	NSO	10869	1177	34647
HD 8574	HIP 6643	NSO	11328	1161	18886
HD 8648	HIP 6653	NSO	11441	987	923
HD 8763	HIP 6732	NSO	11487	117	-42532
HD 8941	HIP 6869	NSO	11171	419	9132
HD 9224	HIP 7090	NSO	11174	507	14937
HD 9280	HIP 7080	NSO	11172	3	41861
HD 9331	HIP 7221	NSO	11933	246	-20086
HD 9407	HIP 7339	NSO	11248	538	-33291
HD 9562	HIP 7276	NSO	11071	1390	-14989
HD 9826	HIP 7513	NSO	8547	2576	-28674
HD 9986	HIP 7585	NSO	11276	987	-21047
HD 10002	HIP 7539	NSO	10973	1119	11562
HD 10086	HIP 7734	NSO	11297	514	2143
HD 10126	HIP 7733	NSO	11301	293	56156
HD 10145	HIP 7902	NSO	11098	1121	17838
HD 10436	HIP 8070	NSO	11469	184	-50957
HD 10476	HIP 7981	NSO	10921	1387	-33647
HD 10697	HIP 8159	NSO	11044	1044	-46022
HD 10700	HIP 8102	NSO	9838	5053	-16619
HD 10780	HIP 8362	NSO	11404	384	2764
HD 11020	HIP 8346	NSO	10999	1081	22786
HD 11226	HIP 8548	NSO	11310	513	10314
HD 11505	HIP 8798	NSO	11279	420	-16470
HD 11964	HIP 9094	NSO	11109	1391	-9366
HD 12051	HIP 9269	NSO	11097	1125	-35102
HD 12235	HIP 9353	NSO	9727	3965	-18434
HD 12414	HIP 9473	NSO	10997	301	15898
HD 12661	HIP 9683	NSO	11463	944	-47310
HD 12846	HIP 9829	NSO	11435	595	-4662
HD 13043	HIP 9911	NSO	11030	1043	-39333
HD 13507	HIP 10321	NSO	11141	397	6172

TABLE 1—Continued

Primary Name (1)	Alternate Name (2)	Ref. (NSO/M) (3)	(JD) (-2440000) (4)	$\Delta T$ (days) (5)	(RV) (m s <sup>-1</sup> ) (6)
HD 13531	HIP 10339	NSO	10979	245	7203
HD 13579	HIP 10531	NSO	11339	293	-12723
HD 13612B	HIP 10303	NSO	11076	1184	-5337
HD 13825	HIP 10505	NSO	11270	432	-2237
HD 13931	HIP 10626	NSO	11265	748	30538
HD 14412	HIP 10798	NSO	11006	1391	7383
HD 15176	HIP 11432	NSO	11494	145	-41783
HD 15335	HIP 11548	NSO	11031	1219	41202
HD 16141	HIP 12048	NSO	11067	1008	-50971
HD 16160	HIP 12114	NSO	9351	3608	25766
HD 16397	HIP 12306	NSO	11060	1082	-99660
HD 16623	HIP 12364	NSO	11088	829	17502
HD 16895	HIP 12777	NSO	8930	2937	24453
HD 17190	HIP 12926	NSO	11146	1186	14138
HD 17230	HIP 12929	NSO	11443	386	11061
HD 17332	HIP 13027	NSO	11481	140	4427
HD 17660	HIP 13258	NSO	11396	324	-28904
HD 17925	HIP 13402	NSO	9385	4084	18068
HD 18143	HIP 13642	NSO	11079	1186	31950
HD 18144	HIP 13601	NSO	11418	386	-1329
HD 18449	HIP 13905	NSO	11487	118	-37021
HD 18632	HIP 13976	NSO	11263	540	28826
HD 18803	HIP 14150	NSO	11210	1426	9878
HD 18907	HIP 14086	NSO	11172	2	42718
HD 19034	HIP 14241	NSO	11082	1186	-20344
HD 19308	HIP 14532	NSO	11234	714	32723
HD 19373	HIP 14632	NSO	7328	532	49449
HD 19467	HIP 14501	NSO	10996	1217	6936
HD 19994	HIP 14954	NSO	9069	4758	19331
HD 20165	HIP 15099	NSO	11070	1186	-16676
HD 20619	HIP 15442	NSO	10941	1178	22689
HD 20630	HIP 15457	NSO	7834	1847	19021
HD 21019	HIP 15776	NSO	10991	1178	41630
HD 21197	HIP 15919	NSO	11145	1186	-13107
HD 21313	HIP 16107	NSO	11901	182	-20017
HD 21847	HIP 16517	NSO	11263	714	30033
HD 22049	HIP 16537	NSO	7147	177	16332
HD 22072	HIP 16641	NSO	11070	1463	11050
HD 22484	HIP 16852	NSO	8391	2301	28080
HD 22879	HIP 17147	NSO	11076	1427	120356
HD 23249	HIP 17378	NSO	11162	1330	-6295
HD 23356	HIP 17420	NSO	11220	501	25287
HD 23439	HIP 17666	NSO	11102	1119	50704
HD 24040	HIP 17960	NSO	11278	954	-9423
HD 24213	HIP 18106	NSO	11181	712	-39608
HD 24238	HIP 18324	NSO	11038	1088	38809
HD 24341	HIP 18309	NSO	11038	1088	142798
HD 24365	HIP 18208	NSO	11092	1088	19278
HD 24451	HIP 18774	NSO	11404	354	17670
HD 24496	HIP 18267	NSO	11236	954	18936
HD 24727	HIP 18388	NSO	11304	954	-18140
HD 24892	HIP 18432	NSO	10952	1217	45410
HD 24916	HIP 18512	NSO	11245	1427	3540
HD 25069	HIP 18606	NSO	11133	1427	38484
HD 25665	HIP 19422	NSO	11436	29	-13546
HD 25680	HIP 19076	NSO	9509	4084	24034
HD 25723	HIP 19011	NSO	11490	144	26748
HD 25918	HIP 19301	NSO	11538	5	-36198
HD 26151	HIP 19232	NSO	11416	412	-6804
HD 26161	HIP 19428	NSO	11236	714	12924
HD 26162	HIP 19388	NSO	11497	116	24776
HD 26767	HIP 19786	NSO	11728	564	38288
HD 26794	HIP 19788	NSO	10980	1131	56573
HD 26965	HIP 19849	NSO	7657	1845	-42331
HD 28005	HIP 20800	NSO	11231	714	34768
HD 28187	HIP 20638	NSO	10990	1215	18321
HD 28343	HIP 20917	M	11476	356	-35073
HD 28344	HIP 20899	NSO	11524	171	39145
HD 28676	HIP 21158	NSO	11305	361	6671
HD 28946	HIP 21272	NSO	11395	386	-46353
HD 29150	HIP 21436	NSO	11396	386	-6615

TABLE 1—Continued

Primary Name (1)	Alternate Name (2)	Ref. (NSO/M) (3)	(JD) (-2440000) (4)	$\Delta T$ (days) (5)	(RV) ( $m s^{-1}$ ) (6)
HD 29528	HIP 21703	NSO	11901	182	-18922
HD 29883	HIP 21988	NSO	11359	385	17843
HD 30562	HIP 22336	NSO	11370	293	77189
HD 30708	HIP 22576	NSO	11209	714	-55738
HD 31253	HIP 22826	NSO	11345	954	12184
HD 31560	HIP 22907	NSO	11162	1217	6203
HD 31966	HIP 23286	NSO	11239	743	-18058
HD 32147	HIP 23311	NSO	9858	4085	21552
HD 32923	HIP 23835	NSO	11305	388	20558
HD 32963	HIP 23884	NSO	11235	715	-62435
HD 33021	HIP 23852	NSO	11070	1216	-22300
HD 33632	HIP 24332	NSO	11182	708	-1707
HD 33636	HIP 24205	NSO	11411	954	5714
HD 33793	HIP 24186	M	11376	410	245194
HD 34411	HIP 24813	NSO	7970	1859	66511
HD 34445	HIP 24681	NSO	11256	743	-78949
HD 34575	HIP 25094	NSO	11731	357	-23520
HD 34721	HIP 24786	NSO	11041	1217	40448
HD 34745	HIP 24864	NSO	11255	743	35376
HD 35627	HIP 25388	NSO	11208	713	27267
HD 35681	HIP 25580	NSO	11195	702	12136
HD 35974	HIP 25490	NSO	11017	1162	76683
HD 36003	HIP 25623	NSO	11214	1215	-55527
HD 36395	HIP 25878	M	10194	4537	8665
HD 37124	HIP 26381	NSO	11203	1164	-23076
HD 37213	HIP 26273	NSO	11088	1163	12464
HD 37394	HIP 26779	NSO	9701	2486	1207
HD 37588	HIP 26689	NSO	10857	0	-58276
HD 37962	HIP 26737	NSO	10899	862	3133
HD 38230	HIP 27207	NSO	11058	1133	-29177
HD 38529	HIP 27253	NSO	11273	1374	30210
HD 38858	HIP 27435	NSO	11017	1133	31543
HD 39715	HIP 27918	NSO	11461	386	-33797
HD 39881	HIP 28066	NSO	11025	1220	333
HD 40397	HIP 28267	NSO	11113	713	143621
HD 40650	HIP 28634	NSO	11030	343	-76840
HD 40979	HIP 28767	NSO	10955	344	32542
HD 42250	HIP 29761	NSO	10908	1119	19715
HD 42581	HIP 29295	M	10801	1579	4724
HD 42618	HIP 29432	NSO	11054	1220	-53501
HD 43523	HIP 30023	NSO	11261	709	-16172
HD 43745	HIP 29843	NSO	10964	1187	-2716
HD 43947	HIP 30067	NSO	11181	714	40545
HD 44420	HIP 30243	NSO	11745	464	-531
HD 44985	HIP 30552	NSO	11227	714	32253
HD 45067	HIP 30545	NSO	11118	1166	47280
HD 45184	HIP 30503	NSO	10940	1220	-3856
HD 45350	HIP 30860	NSO	11819	431	-20727
HD 45391	HIP 30862	NSO	11459	472	-5388
HD 45588	HIP 30711	NSO	10911	1187	35856
HD 46375	HIP 31246	NSO	11491	514	-1032
HD 47127	HIP 31660	NSO	11279	750	49694
HD 47157	HIP 31655	NSO	11549	46	25330
HD 47752	HIP 32010	NSO	11585	90	-44253
HD 48682	HIP 32480	NSO	8280	2301	-23933
HD 48938	HIP 32322	NSO	10927	1134	-10563
HD 49674	HIP 32916	NSO	11963	182	12045
HD 49736	HIP 32874	NSO	11048	708	6687
HD 50281	HIP 32984	NSO	10546	2276	-7082
HD 50499	HIP 32970	NSO	10971	1167	36793
HD 50554	HIP 33212	NSO	11219	709	-3888
HD 50692	HIP 33277	NSO	10965	1119	-15023
HD 50806	HIP 33094	NSO	10870	1187	72388
HD 51219	HIP 33382	NSO	11074	737	-8071
HD 51866	HIP 33852	NSO	11060	1120	-21624
HD 52265	HIP 33719	NSO	11370	745	53810
HD 52456	HIP 33848	NSO	11325	514	-11909
HD 52711	HIP 34017	NSO	9614	4502	24604
HD 53665	HIP 34239	NSO	11232	747	-14703
HD 55575	HIP 35136	NSO	11386	476	84809
HD 56124	HIP 35265	NSO	11324	685	22526

TABLE 1—Continued

Primary Name (1)	Alternate Name (2)	Ref. (NSO/M) (3)	(JD) (-2440000) (4)	$\Delta T$ (days) (5)	(RV) ( $m s^{-1}$ ) (6)
HD 56274	HIP 35139	NSO	10929	1125	66663
HD 56303	HIP 35209	NSO	11164	705	8150
HD 58781	HIP 36249	NSO	11285	744	5013
HD 59747	HIP 36704	NSO	11441	472	-15744
HD 60491	HIP 36827	NSO	11385	410	-9667
HD 61606	HIP 37349	NSO	11255	1163	-18210
HD 63077	HIP 37853	NSO	10415	97	106159
HD 63433	HIP 38228	NSO	11232	703	-15888
HD 63754	HIP 38216	NSO	10867	1132	44973
HD 64090	HIP 38541	NSO	10968	416	-234268
HD 65277	HIP 38931	NSO	11005	1120	-4417
HD 65583	HIP 39157	NSO	10958	1133	14832
HD 66171	HIP 39822	NSO	10944	1119	36412
HD 66428	HIP 39417	NSO	11926	92	44140
HD 67228	HIP 39780	NSO	11431	456	-36012
HD 67458	HIP 39710	NSO	11047	1120	-15686
HD 67767	HIP 40023	NSO	11038	1261	-44318
HD 68017	HIP 40118	NSO	11068	1218	29575
HD 68168	HIP 40133	NSO	11144	746	9162
HD 68978	HIP 40283	NSO	10937	1119	51696
HD 69809	HIP 40761	NSO	11743	422	17534
HD 69897	HIP 40843	NSO	8392	2250	32733
HD 70843	HIP 41226	NSO	11267	795	-13087
HD 71148	HIP 41484	NSO	11177	798	-32342
HD 71334	HIP 41317	NSO	11120	1124	17286
HD 71479	HIP 41479	NSO	11255	742	60217
HD 71881	HIP 41844	NSO	11046	745	13629
HD 72659	HIP 42030	NSO	11255	742	-18253
HD 72673	HIP 41926	NSO	10792	808	14785
HD 72760	HIP 42074	NSO	11386	798	34928
HD 73344	HIP 42403	NSO	11161	468	6097
HD 73350	HIP 42333	NSO	11052	412	35370
HD 73667	HIP 42499	NSO	10981	1091	-12088
HD 74014	HIP 42634	NSO	11462	475	-17089
HD 75332	HIP 43410	NSO	11173	469	4256
HD 75732	HIP 43587	NSO	9301	2513	27351
HD 76151	HIP 43726	NSO	9469	2926	32002
HD 76752	HIP 44089	NSO	11358	798	-12577
HD 76909	HIP 44137	NSO	11725	429	3045
HD 77407	HIP 44458	NSO	10843	23	4827
HD 78366	HIP 44897	NSO	9485	3286	26120
HD 79210	HIP 45343	M	11045	974	11142
HD 79211	HIP 120005	M	11077	974	12495
HD 80367	HIP 45737	NSO	11416	412	51009
HD 82106	HIP 46580	NSO	10970	323	29836
HD 83443	HIP 47202	NSO	11982	167	28994
HD 84035	HIP 47690	NSO	10989	1121	-12225
HD 84737	HIP 48113	NSO	8233	1919	4900
HD 85725	HIP 48468	NSO	10726	752	61610
HD 86728	HIP 49081	NSO	8649	2716	55956
HD 87359	HIP 49350	NSO	11113	737	-260
HD 87424	HIP 49366	NSO	11316	380	-12133
HD 87836	HIP 49680	NSO	11568	96	-42188
HD 87883	HIP 49699	NSO	11311	379	9254
HD 88072	HIP 49756	NSO	11062	737	-17886
HD 88218	HIP 49769	NSO	11010	1261	36652
HD 88230	HIP 49908	M	8883	2897	-25729
HD 88371	HIP 49942	NSO	11006	1089	82497
HD 88725	HIP 50139	NSO	10999	1217	-22045
HD 88986	HIP 50316	NSO	10818	809	29019
HD 89269	HIP 50505	NSO	10979	1164	-7551
HD 89307	HIP 50473	NSO	11074	358	23011
HD 89391	HIP 50478	NSO	11167	1119	29607
HD 90125	HIP 50939	NSO	11054	1286	-13937
HD 90156	HIP 50921	NSO	10899	1162	26934
HD 90711	HIP 51257	NSO	11012	1089	29940
HD 90722	HIP 51258	NSO	11703	423	39984
HD 90839	HIP 51459	NSO	8584	3023	8529
HD 90875	HIP 51468	NSO	11381	383	4948
HD 91204	HIP 51579	NSO	11853	432	-8875
HD 91638	HIP 51784	NSO	11056	381	-4751

TABLE 1—Continued

Primary Name (1)	Alternate Name (2)	Ref. (NSO/M) (3)	(JD) (−2440000) (4)	$\Delta T$ (days) (5)	(RV) (m s <sup>−1</sup> ) (6)
HD 92788	HIP 52409	NSO	11535	924	−4529
HD 92945	HIP 52462	NSO	11323	1218	22856
HD 93745	HIP 52888	NSO	11019	1218	37947
HD 94765	HIP 53486	NSO	11599	93	5525
HD 95128	HIP 53721	NSO	9800	4241	11235
HD 95650	HIP 53985	M	11816	423	−13899
HD 95735	HIP 54035	M	10213	4748	−84689
HD 96418	HIP 54347	NSO	11101	411	−8013
HD 96574	HIP 54383	NSO	11271	57	36055
HD 96700	HIP 54400	NSO	10995	1261	12769
HD 97004	HIP 54614	NSO	11361	293	5352
HD 97037	HIP 54582	NSO	11294	709	−15914
HD 97101	GJ 414A	NSO	10384	2902	−16376
HD 97101B	GJ 414B	M	10307	1930	−15333
HD 97334	HIP 54745	NSO	9429	32734	−3662
HD 97343	HIP 54704	NSO	11051	1261	39794
HD 97658	HIP 54906	NSO	10965	1088	−1654
HD 98281	HIP 55210	NSO	11044	1121	13330
HD 98618	HIP 55459	NSO	11242	865	7058
HD 98697	HIP 55455	NSO	11441	453	−14312
HD 99109	HIP 55664	NSO	11478	534	32997
HD 99491	HIP 55846	NSO	11047	1286	4190
HD 99492	HIP 55848	NSO	11110	1243	3726
HD 100180	HIP 56242	NSO	11017	1284	−4854
HD 100623	HIP 56452	NSO	11003	1162	−21959
HD 101177	HIP 56809	NSO	11461	386	−16912
HD 101259	HIP 56830	NSO	11077	1121	96905
HD 101501	HIP 56997	NSO	7992	2213	−5565
HD 102158	HIP 57349	NSO	11009	1121	28122
HD 102634	HIP 57629	NSO	11099	381	1254
HD 102870	HIP 57757	NSO	7466	1058	4448
HD 103095	HIP 57939	NSO	11289	153	−98073
HD 103432	HIP 58067	NSO	11033	1241	6079
HD 103932	HIP 58345	NSO	11114	1218	48499
HD 104067	HIP 58451	NSO	11247	1218	15021
HD 104526	HIP 58698	NSO	10539	143	4635
HD 104556	HIP 58708	NSO	11057	1240	−10678
HD 104800	HIP 58843	NSO	11820	547	9989
HD 105113	HIP 59021	NSO	11070	1218	31871
HD 105405	HIP 59175	NSO	11412	325	2196
HD 105590	HIP 59272	NSO	10733	494	1976
HD 105618	HIP 59278	NSO	11957	219	7466
HD 105631	HIP 59280	NSO	11033	1240	−2428
HD 106116	HIP 59532	NSO	11063	1241	14543
HD 106156	HIP 59572	NSO	11063	1240	−7415
HD 107148	HIP 60081	NSO	11890	548	25216
HD 107705	HIP 60353	NSO	11278	797	4759
HD 108510	HIP 60816	NSO	11207	0	6888
HD 108874	HIP 61028	NSO	11521	339	−30137
HD 109358	HIP 61317	NSO	11735	480	6259
HD 110315	HIP 61901	NSO	11108	1242	24604
HD 110537	HIP 62039	NSO	11386	748	35461
HD 111031	HIP 62345	NSO	11051	1243	−20458
HD 111066	HIP 62349	NSO	11351	330	6407
HD 111398	HIP 62536	NSO	11411	331	3154
HD 111484	HIP 62596	NSO	11408	721	−20643
HD 111484B	SAO 119612	NSO	11387	721	−19377
HD 111515	HIP 62607	NSO	11059	1243	2548
HD 111631	HIP 62687	M	11901	517	5041
HD 112257	HIP 63048	NSO	11044	473	−39428
HD 114174	HIP 64150	NSO	11083	1119	24002
HD 114710	HIP 64394	NSO	7397	1058	5295
HD 114729	HIP 64459	NSO	11380	1244	64925
HD 114783	HIP 64457	NSO	11551	772	−12012
HD 114946	HIP 64577	NSO	11118	1242	−48181
HD 115383	HIP 64792	NSO	8623	2511	−27138
HD 115589	HIP 64905	NSO	11434	505	−21614
HD 115617	HIP 64924	NSO	9770	0	−7850
HD 116442	HIP 65352	NSO	11301	1242	28421
HD 116443	HIP 65355	NSO	11155	1242	27416
HD 117207	HIP 65808	NSO	11199	1240	−17476

TABLE 1—Continued

Primary Name (1)	Alternate Name (2)	Ref. (NSO/M) (3)	(JD) (−2440000) (4)	$\Delta T$ (days) (5)	(RV) (m s <sup>−1</sup> ) (6)
HD 117936	HIP 66147	NSO	11404	720	−6086
HD 118914	HIP 66621	NSO	11950	307	16460
HD 119850	HIP 67155	M	10336	2856	15809
HD 120066	HIP 67246	NSO	11205	1241	−30561
HD 120467	HIP 67487	NSO	11252	1157	−37806
HD 120476	HIP 67422	NSO	11492	392	−20380
HD 121560	HIP 68030	NSO	11016	23	−10532
HD 122064	HIP 68184	NSO	11958	548	−26471
HD 122120	HIP 68337	NSO	11130	1157	−57444
HD 122303	HIP 68469	M	11497	172	−25813
HD 122652	HIP 68593	NSO	11177	675	1409
HD 124106	HIP 69357	NSO	11117	1396	3288
HD 124292	HIP 69414	NSO	11104	474	37773
HD 124642	HIP 69526	NSO	11585	89	−16242
HD 124694	HIP 69518	NSO	11016	22	−14644
HD 125184	HIP 69881	NSO	11184	1403	−12377
HD 125455	HIP 70016	NSO	11154	1404	−9806
HD 126053	HIP 70319	NSO	10208	4746	−19241
HD 126614	HIP 70623	NSO	11485	480	−33086
HD 126961	HIP 70782	NSO	11050	202	−5839
HD 127334	HIP 70873	NSO	11129	533	−405
HD 128167	HIP 71284	NSO	8333	2080	141
HD 128311	HIP 71395	NSO	11392	696	−9569
HD 128428	HIP 71462	NSO	11063	795	−42074
HD 129010	HIP 71774	NSO	11149	1158	−8137
HD 129191	HIP 71803	NSO	11827	479	12685
HD 130087	HIP 72190	NSO	11835	483	−15673
HD 130307	HIP 72312	NSO	11218	1429	12864
HD 130322	HIP 72339	NSO	12038	407	−12441
HD 130871	HIP 72577	NSO	11147	1429	−32159
HD 130948	HIP 72567	NSO	9090	3698	−2502
HD 130992	HIP 72688	NSO	11256	1134	−57160
HD 131117	HIP 72772	NSO	11105	1242	−28834
HD 131156A	GJ 566A	NSO	7325	1157	1303
HD 131156B	GJ 566B	NSO	9090	3609	3274
HD 131509	HIP 72830	NSO	11090	1133	−44625
HD 131977	HIP 73184	NSO	10272	1407	26961
HD 132142	HIP 73005	NSO	11094	1158	−14771
HD 132375	HIP 73309	NSO	11139	624	−24370
HD 133161	HIP 73593	NSO	11181	796	−32628
HD 134044	HIP 73941	NSO	11222	624	−5874
HD 134439	HIP 74235	NSO	11090	820	310084
HD 134440	HIP 74234	NSO	11365	692	310614
HD 134987	HIP 74500	NSO	10962	952	5038
HD 135101	HIP 74432	NSO	11259	1480	−38921
HD 135599	HIP 74702	NSO	11108	468	−3149
HD 136442	HIP 75101	NSO	11483	720	−46935
HD 136654	HIP 75104	NSO	11020	21	−27029
HD 136713	HIP 75253	NSO	11090	1428	−6037
HD 136834	HIP 75266	NSO	10982	1403	−26374
HD 136923	HIP 75277	NSO	11196	798	−7042
HD 136925	HIP 75281	NSO	11253	842	−48942
HD 137778	HIP 75722	NSO	11234	1479	7752
HD 138549	HIP 76200	NSO	11100	1158	12024
HD 138573	HIP 76114	NSO	11221	625	−35691
HD 138776	HIP 76228	NSO	11509	368	10674
HD 139323	HIP 76375	NSO	11092	1134	−67101
HD 139457	HIP 76543	NSO	11427	338	37708
HD 139477	HIP 76315	NSO	11387	453	−8893
HD 141004	HIP 77257	NSO	8789	3560	−66416
HD 141103	HIP 77335	NSO	11106	358	−48258
HD 142373	HIP 77760	NSO	8418	3561	−56107
HD 142860	HIP 78072	NSO	7746	1327	6544
HD 143291	HIP 78241	NSO	11065	1428	−72474
HD 143761	HIP 78459	NSO	10900	1149	17949
HD 144179	HIP 78842	NSO	10875	436	−24253
HD 144579	HIP 78775	NSO	11094	1158	−59431
HD 144585	HIP 78955	NSO	11112	1158	−14067
HD 144988	HIP 79214	NSO	11116	1208	−53211
HD 145229	HIP 79165	NSO	11100	359	−36204
HD 145435	HIP 79152	NSO	11086	359	−42685

TABLE 1—Continued

Primary Name (1)	Alternate Name (2)	Ref. (NSO/M) (3)	(JD) (-2440000) (4)	$\Delta T$ (days) (5)	(RV) ( $m s^{-1}$ ) (6)
HD 145675.....	HIP 79248	NSO	11307	1150	-13693
HD 145809.....	HIP 79524	NSO	11088	1428	21146
HD 145897.....	HIP 79540	NSO	11457	301	-23611
HD 145934.....	SAO 102017	NSO	11342	1101	-27954
HD 145958.....	HIP 79492	NSO	11183	1518	18422
HD 146233.....	HIP 79672	NSO	11245	1088	11748
HD 146362.....	GJ 615.2B	NSO	11121	1134	-14855
HD 146775.....	HIP 79946	NSO	11116	1245	-30218
HD 147044.....	HIP 79862	NSO	11339	746	-14560
HD 147231.....	HIP 79619	NSO	11182	1157	-16461
HD 147379.....	HIP 79755	M	12021	482	-18789
HD 147379B.....	GJ 617B	M	12040	482	-18530
HD 147776.....	HIP 80366	NSO	11541	265	7341
HD 148467.....	HIP 80644	NSO	11686	124	-36207
HD 148513.....	HIP 80693	NSO	11443	299	7723
HD 149200.....	HIP 81062	NSO	11017	22	-7176
HD 149652.....	HIP 81279	NSO	11080	359	-31167
HD 149661.....	HIP 81300	NSO	10107	3304	-12857
HD 149806.....	HIP 81375	NSO	11358	747	10391
HD 150433.....	HIP 81681	NSO	11122	1065	-40215
HD 150698.....	HIP 81910	NSO	11073	1131	48229
HD 150933.....	HIP 81880	NSO	11287	747	-27880
HD 151101.....	HIP 81660	NSO	11551	455	-1329
HD 151288.....	HIP 82003	M	10162	4746	-31357
HD 151541.....	HIP 81813	NSO	11067	1158	9475
HD 151877.....	HIP 82267	NSO	11082	1160	2033
HD 151995.....	HIP 82389	NSO	11145	1429	-5557
HD 152391.....	HIP 82588	NSO	10746	2588	45066
HD 152446.....	HIP 82568	NSO	11142	387	-42504
HD 152792.....	HIP 82636	NSO	11093	1159	4759
HD 153458.....	HIP 83181	NSO	11258	842	641
HD 153627.....	HIP 83204	NSO	11306	770	-1462
HD 153834.....	HIP 83254	NSO	11446	275	10821
HD 154088.....	HIP 83541	NSO	11071	1131	14180
HD 154345.....	HIP 83389	NSO	11103	1159	-46930
HD 154363.....	HIP 83591	NSO	11178	1403	34146
HD 154417.....	HIP 83601	NSO	11331	63	-16739
HD 155060.....	HIP 83827	NSO	11175	747	-10542
HD 155423.....	HIP 84082	NSO	11367	747	-33561
HD 156026.....	HIP 84478	NSO	11367	772	153
HD 156365.....	HIP 84636	NSO	11089	1163	-13136
HD 156681.....	HIP 84671	NSO	11427	301	38842
HD 156826.....	HIP 84801	NSO	11267	1431	-32634
HD 157214.....	HIP 84862	NSO	8668	3650	-78546
HD 157338.....	HIP 85158	NSO	11072	1155	-24315
HD 157347.....	HIP 85042	NSO	11256	748	-35901
HD 157466.....	HIP 85007	NSO	11399	800	34125
HD 157617.....	HIP 85139	NSO	11455	268	13119
HD 157881.....	HIP 85295	M	11130	1427	-23199
HD 159063.....	HIP 85799	NSO	11179	690	-6385
HD 159222.....	HIP 85810	NSO	11144	1249	-51605
HD 159501.....	HIP 85888	NSO	11470	248	-30123
HD 159909.....	HIP 86193	NSO	11212	748	-76809
HD 160693.....	HIP 86431	NSO	11076	1157	34084
HD 161555.....	HIP 86985	NSO	11123	358	72021
HD 161848.....	HIP 87089	NSO	11064	1428	-94929
HD 162826.....	HIP 87382	NSO	11216	625	1848
HD 163102.....	HIP 87678	NSO	11093	358	-26920
HD 163153.....	HIP 87710	NSO	11234	750	-73024
HD 163489.....	GJ 4035	NSO	11135	1163	-49364
HD 164507.....	HIP 88217	NSO	11265	824	5370
HD 164595.....	HIP 88194	NSO	11249	748	2020
HD 164922.....	HIP 88348	NSO	11196	1520	20248
HD 165222.....	HIP 88574	M	10299	4747	32671
HD 165438.....	HIP 88684	NSO	11457	274	-26747
HD 165567.....	HIP 88533	NSO	11202	382	3853
HD 165634.....	HIP 88839	NSO	11394	83	-4867
HD 165683.....	HIP 88636	NSO	11426	32	-546
HD 166620.....	HIP 88972	NSO	9370	3649	-19418
HD 167389.....	HIP 89282	NSO	11254	749	-5545
HD 168009.....	HIP 89474	NSO	11329	747	-64595

TABLE 1—Continued

Primary Name (1)	Alternate Name (2)	Ref. (NSO/M) (3)	(JD) (-2440000) (4)	$\Delta T$ (days) (5)	(RV) ( $m s^{-1}$ ) (6)
HD 168723.....	HIP 89962	NSO	8930	2734	9371
HD 168746.....	HIP 90004	NSO	12060	406	-25603
HD 169191.....	HIP 90067	NSO	11414	127	-19268
HD 169830.....	HIP 90485	NSO	12036	406	-17304
HD 170174.....	SAO 123515	NSO	11177	1208	-28841
HD 170469.....	HIP 90593	NSO	11954	457	-59423
HD 170493.....	HIP 90656	NSO	11147	1480	-54752
HD 170657.....	HIP 90790	NSO	10812	2173	-43131
HD 170778.....	HIP 90586	NSO	11307	744	-22670
HD 171067.....	HIP 90864	NSO	11058	1479	-46252
HD 171665.....	HIP 91287	NSO	11040	1421	-23259
HD 171918.....	HIP 91332	NSO	11902	394	-67256
HD 172051.....	HIP 91438	NSO	11149	1421	37103
HD 172310.....	HIP 91381	NSO	11189	1038	30997
HD 172513.....	HIP 91700	NSO	11397	1248	-11545
HD 172649.....	HIP 91507	NSO	11016	23	-11419
HD 173701.....	HIP 91949	NSO	11071	1158	-45602
HD 173739.....	HIP 91768	M	11078	1104	-834
HD 173740.....	HIP 91772	M	11078	1104	1187
HD 173818.....	HIP 92200	NSO	11499	443	15544
HD 174912.....	HIP 92532	NSO	11301	418	-13083
HD 174947.....	HIP 92747	NSO	11424	106	-7100
HD 175541.....	HIP 92895	NSO	11075	1422	19698
HD 175726.....	HIP 92984	NSO	11025	44	10277
HD 176377.....	HIP 93185	NSO	11232	825	-40611
HD 176982.....	HIP 93518	NSO	11037	1419	-6793
HD 177153.....	HIP 93427	NSO	11290	746	-14953
HD 177830.....	HIP 93746	NSO	11183	1213	-72173
HD 179949.....	HIP 94645	NSO	11940	370	-24662
HD 179957.....	GJ 9648B	NSO	11072	1158	-41822
HD 179958.....	GJ 9648A	NSO	11029	1158	-41158
HD 180617.....	HIP 94761	M	9359	3609	35880
HD 180684.....	HIP 94751	NSO	11542	420	-2615
HD 181234.....	HIP 95015	NSO	11510	451	-46783
HD 181655.....	HIP 94981	NSO	11249	897	2036
HD 182488.....	HIP 95319	NSO	11022	41	-21508
HD 182572.....	HIP 95447	NSO	11151	1340	-100292
HD 183341.....	HIP 95772	NSO	11206	748	-40888
HD 183650.....	HIP 95821	NSO	11075	1158	-9744
HD 183658.....	HIP 95962	NSO	11228	748	58176
HD 183870.....	HIP 96085	NSO	11295	1517	-48864
HD 184385.....	HIP 96183	NSO	11106	441	11406
HD 185144.....	HIP 96100	NSO	9977	3998	26691
HD 185295.....	SAO 124877	NSO	11135	1339	-18575
HD 185351.....	HIP 96459	NSO	11426	148	-5886
HD 185720.....	HIP 96813	NSO	11027	41	15992
HD 186408.....	HIP 96895	NSO	9256	3651	-27377
HD 186427.....	HIP 96901	NSO	8634	2644	-27871
HD 187123.....	HIP 97336	NSO	11032	269	-16954
HD 187237.....	HIP 97420	NSO	11223	749	-32962
HD 187897.....	HIP 97779	NSO	11243	701	-37568
HD 187923.....	HIP 97767	NSO	10926	1426	-20611
HD 188015.....	HIP 97769	NSO	11987	379	68
HD 188510.....	HIP 98020	NSO	11563	452	-192444
HD 188512.....	HIP 98036	NSO	8769	3648	-40109
HD 189067.....	HIP 98206	NSO	11119	413	-10922
HD 189625.....	HIP 98589	NSO	11268	988	-28218
HD 190007.....	HIP 98698	NSO	11225	810	-30303
HD 190067.....	HIP 98677	NSO	11009	1517	20385
HD 190360.....	HIP 98767	NSO	11189	1340	-45308
HD 190404.....	HIP 98792	NSO	10990	1479	-2527
HD 191022.....	HIP 98978	NSO	11093	441	-12842
HD 191785.....	HIP 99452	NSO	10947	1427	-49286
HD 192020.....	GJ 4138	NSO	11118	1207	-11366
HD 192263.....	HIP 99711	NSO	11346	810	-10738
HD 192343.....	HIP 99727	NSO	11781	1767	-526
HD 192344.....	HIP 99729	NSO	12075	407	-451
HD 193017.....	HIP 100072	NSO	11084	443	15584
HD 193202.....	HIP 99427	NSO	11355	26	-1623
HD 193795.....	HIP 100363	NSO	11976	369	6921
HD 193901.....	HIP 100568	NSO	11593	296	-171455

TABLE 1—Continued

Primary Name (1)	Alternate Name (2)	Ref. (NSO/M) (3)	(JD) (-2440000) (4)	$\Delta T$ (days) (5)	(RV) ( $m s^{-1}$ ) (6)
HD 194035.....	HIP 100500	NSO	11252	444	16665
HD 194766.....	HIP 100895	NSO	11101	412	-15131
HD 195104.....	HIP 101059	NSO	11022	22	-14936
HD 195564.....	HIP 101345	NSO	11141	1428	9535
HD 196201.....	HIP 101597	NSO	11431	426	-19821
HD 196761.....	HIP 101997	NSO	11023	1478	-41987
HD 196850.....	HIP 101875	NSO	11196	1207	-21045
HD 196885.....	HIP 101966	NSO	11152	441	-30189
HD 197076.....	HIP 102040	NSO	11035	1389	-35409
HD 197139.....	HIP 101986	NSO	11437	125	-24024
HD 198089.....	HIP 102610	NSO	11158	441	-33434
HD 198802.....	HIP 103077	NSO	11104	1101	-3171
HD 199305.....	HIP 103096	M	11164	1077	-17161
HD 199476.....	HIP 102970	NSO	11040	765	-30230
HD 199598.....	HIP 103455	NSO	11354	747	-25301
HD 199960.....	HIP 103682	NSO	11054	1338	-17605
HD 200538.....	HIP 104071	NSO	10991	1389	15377
HD 200746.....	HIP 104075	NSO	11408	67	13807
HD 201091.....	HIP 104214	NSO	7369	1066	-65726
HD 201092.....	HIP 104217	M	8258	2297	-64023
HD 202108.....	HIP 104733	NSO	11258	747	2502
HD 202573.....	HIP 105000	NSO	10823	799	-26179
HD 202575.....	HIP 105038	NSO	11175	1337	-18065
HD 202751.....	HIP 105152	NSO	11054	1338	-27427
HD 203644.....	HIP 105497	NSO	11436	75	-4356
HD 204587.....	HIP 106147	M	11004	1338	-84186
HD 206332.....	HIP 107040	NSO	11254	746	-44542
HD 206387.....	HIP 107107	NSO	11807	821	-7761
HD 206860.....	HIP 107350	NSO	8929	2894	-16833
HD 207804.....	HIP 107840	NSO	10636	63	-14848
HD 207874.....	HIP 107941	NSO	11243	720	-26702
HD 208313.....	HIP 108156	NSO	11509	335	-13251
HD 208801.....	HIP 108506	NSO	10595	2552	-50179
HD 209128.....	HIP 108691	NSO	11432	144	8115
HD 209290.....	HIP 108782	M	11425	30	18363
HD 209458.....	HIP 108859	NSO	11586	414	-14759
HD 209747.....	HIP 109068	NSO	11404	127	-18889
HD 209761.....	HIP 109023	NSO	11443	105	-28712
HD 209875.....	HIP 109144	NSO	11208	750	-40896
HD 210277.....	HIP 109378	NSO	10756	766	-20873
HD 210302.....	HIP 109422	NSO	11472	363	-16259
HD 210392.....	HIP 109428	NSO	11972	369	-1496
HD 210460.....	HIP 109439	NSO	10843	1093	20429
HD 210667.....	HIP 109527	NSO	11175	435	-19443
HD 210752.....	HIP 109646	NSO	11157	390	57225
HD 210762.....	HIP 109602	NSO	11438	93	-8799
HD 211038.....	HIP 109822	NSO	10807	796	10407
HD 212801.....	HIP 110853	NSO	11021	1389	-8475
HD 213119.....	HIP 110986	NSO	11407	81	-30288
HD 213519.....	HIP 111148	NSO	11247	949	-31630
HD 213575.....	HIP 111274	NSO	11282	449	-21544
HD 213628.....	HIP 111349	NSO	10939	1003	-50445
HD 214557.....	HIP 111748	NSO	11177	443	-38534
HD 214749.....	HIP 111960	NSO	10984	1165	1
HD 214868.....	HIP 111944	NSO	11404	128	-10881
HD 214995.....	HIP 112067	NSO	11439	93	-28855
HD 215152.....	HIP 112190	NSO	11345	783	-13795
HD 215648.....	HIP 112447	NSO	8320	1809	-5856
HD 216259.....	HIP 112870	NSO	10981	1517	1291
HD 216625.....	HIP 113086	NSO	11020	23	10993
HD 216646.....	HIP 113084	NSO	11435	93	-7670
HD 216899.....	HIP 113296	M	11166	1127	-27317
HD 217004.....	HIP 113386	NSO	11015	1072	371
HD 217014.....	HIP 113357	NSO	10005	9	-33225
HD 217107.....	HIP 113421	NSO	11199	700	-13399
HD 217165.....	HIP 113438	NSO	11496	452	15391
HD 217357.....	HIP 113576	M	11087	1074	16420
HD 217459.....	HIP 113622	NSO	11446	137	18630
HD 217563.....	HIP 113686	NSO	11448	96	4661
HD 217618.....	HIP 113695	NSO	11515	334	-12730
HD 217813.....	HIP 113829	NSO	11423	31	2030

TABLE 1—Continued

Primary Name (1)	Alternate Name (2)	Ref. (NSO/M) (3)	(JD) (-2440000) (4)	$\Delta T$ (days) (5)	(RV) ( $m s^{-1}$ ) (6)
HD 217877.....	HIP 113896	NSO	11182	442	-12676
HD 217987.....	HIP 114046	M	11139	385	8809
HD 218029.....	HIP 113864	NSO	11427	106	-8708
HD 218133.....	HIP 114028	NSO	11147	443	-48799
HD 218209.....	HIP 113989	NSO	11114	1040	-15895
HD 218566.....	HIP 114322	NSO	11028	1186	-37804
HD 218730.....	HIP 114424	NSO	11160	442	2009
HD 218739.....	HIP 114385	NSO	11006	0	-5681
HD 218792.....	HIP 114449	NSO	11423	105	2548
HD 218868.....	HIP 114456	NSO	11193	442	-30622
HD 219134.....	HIP 114622	NSO	10206	672	-18558
HD 219172.....	HIP 114670	NSO	11137	419	-2828
HD 219538.....	HIP 114886	NSO	11096	1090	9990
HD 219834B.....	HIP 115125	NSO	11301	1427	10782
HD 221354.....	HIP 115194	NSO	10989	1517	-48118
HD 220339.....	HIP 115445	NSO	11132	1389	34001
HD 220957.....	HIP 115839	NSO	10427	97	-81264
HD 221146.....	HIP 115951	NSO	11100	439	-15137
HD 221354.....	HIP 116085	NSO	11410	336	-25113
HD 221356.....	HIP 116106	NSO	10925	1479	-12713
HD 221830.....	HIP 116421	NSO	11211	444	-112299
HD 222033.....	HIP 116542	NSO	11195	443	-13088
HD 222134.....	HIP 116613	NSO	11152	793	-169
HD 222368.....	HIP 116771	NSO	7945	1787	5656
HD 222582.....	HIP 116906	NSO	11315	950	12067
HD 223238.....	HIP 117367	NSO	11216	950	-15420
HD 223498.....	HIP 117526	NSO	11031	1185	-23985
HD 223559.....	HIP 117567	NSO	11465	117	-62839
HD 223691.....	HIP 117668	NSO	10999	704	1656
HD 223807.....	HIP 117756	NSO	11483	116	-15825
HD 224156.....	HIP 117953	NSO	11482	117	14883
HD 224383.....	HIP 118115	NSO	11146	633	-31205
HD 225216.....	HIP 379	NSO	11476	117	-28860
HD 225261.....	HIP 400	NSO	11105	1389	7511
HD 230409.....	HIP 93341	NSO	11578	346	-2238
HD 230999.....	HIP 94615	NSO	11930	335	-81527
HD 232979.....	HIP 21553	M	11693	356	34401
HD 233641.....	HIP 46639	NSO	11935	92	36182
HD 239960.....	HIP 110893	M	11146	833	-33937
HD 245409.....	HIP 26335	M	11002	1161	22046
HD 260655.....	HIP 31635	M	11181	713	-58178
HD 265866.....	HIP 33226	M	10225	2907	22914
HD 281540.....	HIP 19143	NSO	11515	170	110217
HD 285968.....	HIP 21932	M	11238	742	26219
HD 349726.....	HIP 93873	M	11304	723	32407
GJ 2.....	HIP 428	M	12055	405	-240
GJ 4A.....	HIP 473	M	11979	405	1669
GJ 4B.....	BD +45 4408B	M	12067	432	-1655
GJ 14.....	HIP 1368	M	9537	3745	2957
GJ 26.....	G132-11	M	12030	608	-347
GJ 47.....	G243-50	M	11852	551	7574
GJ 48.....	HIP 4856	M	11159	866	1500
GJ 49.....	HIP 4872	M	11083	877	-5966
GJ 54.1.....	HIP 5643	M	11263	532	28089
GJ 70.....	HIP 8051	M	11867	552	-25883
GJ 83.1.....	G73-12	M	11566	383	-28567
GJ 96.....	HIP 11048	M	11890	607	-37941
GJ 107B.....	BD +48 746B	M	9713	3608	25765
GJ 109.....	HIP 12781	M	11522	173	30568
GJ 156.....	HIP 18280	M	10978	1089	62597
GJ 173.....	HIP 21556	M	11788	319	-6768
GJ 226.....	HIP 29277	M	11126	741	-1622
GJ 273.....	HIP 36208	M	10129	3167	18216
GJ 273.1.....	HIP 36357	NSO	11155	0	-3951
GJ 357.....	HIP 47103	M	11204	743	-34581
GJ 361.....	HIP 47513	M	11753	391	11511
GJ 362.....	HIP 47650	M	11777	393	6606
GJ 373.....	HIP 48714	M	11703	422	15493
GJ 382.....	HIP 49986	M	11053	974	7932
GJ 388.....	SAO 81292	M	9343	3135	12420
GJ 390.....	HIP 51007	M	11818	428	21590



TABLE 1—Continued

Primary Name (1)	Alternate Name (2)	Ref. (NSO/M) (3)	(JD) (−2440000) (4)	ΔT (days) (5)	(RV) (m s <sup>−1</sup> ) (6)
GJ 393.....	HIP 51317	M	11020	936	8335
GJ 397.....	HIP 51525	M	11323	351	21052
GJ 402.....	HIP 53020	M	11776	513	−1042
GJ 406.....	G45-20	M	11316	380	19482
GJ 408.....	HIP 53767	M	11133	975	3151
GJ 412A.....	HIP 54211	M	10386	2903	68886
GJ 413.1.....	HIP 54532	M	11759	456	−3830
GJ 424.....	HIP 55360	M	11796	513	60401
GJ 433.....	HIP 56528	M	11419	383	17973
GJ 436.....	HIP 57087	M	11778	513	9607
GJ 445.....	HIP 57544	M	11227	863	−111654
GJ 447.....	HIP 57548	M	11362	722	−31087
GJ 450.....	HIP 57802	M	11247	863	273
GJ 465.....	HIP 60559	M	11764	455	51174
GJ 486.....	HIP 62452	M	11146	867	19090
GJ 514.....	HIP 65859	M	11085	1158	14556
GJ 519.....	HIP 66459	M	11827	482	−14557
GJ 528B.....	BD +27 2296B	NSO	11519	369	−22896
GJ 553.1.....	HIP 70975	M	11882	520	−1756
GJ 555.....	HIP 71253	M	11496	171	−1453
GJ 569.....	HIP 72944	M	9424	1336	−7209
GJ 581.....	HIP 74995	M	11498	176	−9398
GJ 615.1B.....	BD +13 3091B	NSO	11244	1520	18427
GJ 625.....	HIP 80459	M	11224	842	−13034
GJ 628.....	HIP 80824	M	11759	688	−21222
GJ 649.....	HIP 83043	M	12002	780	4316
GJ 667C.....	...	M	11982	458	6353
GJ 671.....	HIP 84790	M	12056	457	−19528
GJ 678.1A.....	HIP 85665	M	11218	749	−12457
GJ 686.....	HIP 86287	M	11149	1099	−9515
GJ 687.....	HIP 86162	M	11173	1101	−28779
GJ 694.....	HIP 86776	M	11250	748	−14269
GJ 699.....	HIP 87937	M	10418	4022	−110506
GJ 729.....	HIP 92403	M	11397	721	−10499
GJ 745B.....	HIP 93899	M	11304	723	32171
GJ 793.....	HIP 101180	M	11209	401	10599
GJ 806.....	HIP 102401	M	9736	4037	−24702
GJ 821.....	HIP 104432	M	12001	430	−58267

TABLE 1—Continued

Primary Name (1)	Alternate Name (2)	Ref. (NSO/M) (3)	(JD) (−2440000) (4)	ΔT (days) (5)	(RV) (m s <sup>−1</sup> ) (6)
GJ 849.....	HIP 109388	M	10972	834	−15256
GJ 905.....	G171-10	M	11248	542	−77949
GJ 908.....	HIP 117473	M	10076	4505	−71147
GJ 1005.....	HIP 1242	M	11044	60	−26425
GJ 1148.....	HIP 57050	M	11834	484	−9095
GJ 2066.....	HIP 40501	M	11042	744	62205
GJ 2130A.....	HIP 86961	M	12007	460	−28990
GJ 3126.....	G244-47	M	11872	551	−84115
GJ 3709B.....	...	M	11786	426	−9226
GJ 3804.....	HIP 67164	M	11910	517	4969
GJ 3897B.....	HIP 74434	NSO	11213	1306	−38829
GJ 3992.....	HIP 84099	M	11928	419	−44443
GJ 4048A.....	G204-58	M	11994	458	477
GJ 4062.....	G205-28	M	11940	423	−19003
GJ 4063.....	...	M	11519	296	12495
GJ 4070.....	HIP 91699	M	12021	456	−31764
GJ 4098.....	G207-19	M	12025	423	−1730
GJ 4333.....	HIP 115332	M	12042	229	−6507
GJ 9492.....	HIP 71898	M	11184	864	18704
HIP 795.....	BD +07 9s	NSO	11419	208	14685
HIP 5004.....	G269-87	NSO	11865	547	45733
HIP 10449.....	SAO 129772	NSO	11481	140	28116
HIP 15904.....	BD +11 468	NSO	11668	249	86739
HIP 52942.....	SAO 99310	NSO	11425	536	24574
HIP 59406.....	...	M	11745	392	−9100
HIP 80295.....	BD −11 4126	NSO	11455	395	−17315
HIP 89215.....	BD +05 3640	NSO	11795	689	−1050
HIP 103039.....	...	M	11239	747	16300
HIP 103269.....	BD +41 3931	NSO	11531	336	−130673
HIP 106924.....	BD +59 2407	NSO	11640	296	−244634
BD +18 4505C.....	...	NSO	11999	722	−89693
BD −10 3166.....	...	NSO	11499	533	26679
G161-29.....	...	NSO	11448	413	22370
G195-59.....	...	M	11782	401	−3451
G60-06.....	...	NSO	11418	533	−18105

NOTE.— Table 1 is also available in machine-readable form in the electronic edition of the *Astrophysical Journal Supplement*.  
<sup>a</sup> Stars with  $\sigma_{\text{rms}} < 100 \text{ m s}^{-1}$ .

these instantaneous velocities.<sup>6</sup> Four observations of the day sky and two observations of Vesta were analyzed with the before mentioned Doppler method using the NSO solar spectrum. These references showed that our raw velocities, from Keck and Lick, were consistently large by  $522 \pm 5 \text{ m s}^{-1}$ .

There are various possible sources for the  $522 \text{ m s}^{-1}$  offset in our raw velocities. The absolute wavelength scales of both the NSO solar spectrum and our FTS iodine spectrum are not well known. According to Kurucz et al. (1984), the solar lines are broadened by  $200 \text{ m s}^{-1}$  due to the change in the radial velocity during the observation, and the wavelengths may have errors as large as  $100 \text{ m s}^{-1}$ . The wavelength scale of the iodine FTS spectrum comes from the calibration made at the McMath telescope at Kitt Peak. We have no independent way to verify the integrity of the zero point in wavelength of this FTS iodine spectrum. The third concern stems from the instrumental profile of the HIRES and the Hamilton spectrometers. It is known that the PSF is asymmetric to some degree (Valenti et al. 1995) and may give rise to systematic velocity shifts. However, it is unlikely that the same asymmetry in the same direction would be found at

two different spectrometers. Therefore, we consider this possibility less plausible.

All Doppler measurements which used the NSO solar spectrum as the reference template were corrected for this offset of  $522 \text{ m s}^{-1}$ . Since currently no M dwarfs exist having a definitive barycentric radial velocity, the velocity zero point for the M stars in our sample was set using the previously published velocities for the five standards from Marcy et al. (1987), which have errors of  $\sim 0.4 \text{ km s}^{-1}$ .

## 6. COMPARISON OF PRESENT VELOCITIES WITH STANDARD STARS

To get an external measure of the accuracy of our barycentric radial velocities we have compared our velocities to published velocities of supposed radial velocity standard stars. We carry out this comparison separately for the FGK stars and for the M stars.

### 6.1. F, G, and K Stars

We compared our velocities to those of the 26 standard stars that were measured by Udry et al. (1999a). The results of this comparison are shown in Figures 2 and 3 and yield  $\langle V_{\text{Udry}} - V_{\text{Present}} \rangle = -53 \text{ m s}^{-1}$ , with an rms scatter of

<sup>6</sup> See <http://ssd.jpl.nasa.gov/cgi-bin/eph>.

TABLE 2  
 RADIAL VELOCITIES: STARS WITH  $rms > 0.1 \text{ km s}^{-1a}$

Primary Name (1)	Alternate Name (2)	Ref. (NSO/M) (3)	JD (-2440000) (4)	RV ( $\text{m s}^{-1}$ ) (5)	$\langle \text{JD} \rangle$ (-2440000) (6)	$\Delta T$ (days) (7)	$\sigma_{rms}$ ( $\text{m s}^{-1}$ ) (8)	$N$ (9)	Comment (10)
HD 1854 .....	SAO 192490	NSO	10984.112	24327	10714	119	3651	4	
HD 3346 .....	HIP 2900	NSO	10012.747	-33377	9317	2220	172	29	
HD 3770 .....	HIP 3169	NSO	11774.903	-8124	11555	1132	178	13	L
HD 3795 .....	HIP 3185	NSO	11756.021	-46595	11131	1535	156	24	L
HD 4271 .....	HIP 3540	NSO	11047.927	32566	11037	21	7799	2	
HD 4747 .....	HIP 3850	NSO	11756.051	10399	11092	1731	315	21	CO
HD 7483 .....	HIP 5881	NSO	12129.043	-17717	12015	515	2602	11	CO
HD 8331 .....	HIP 6442	NSO	11154.627	-12270	11091	128	2349	2	
HD 9770 .....	HIP 7372	NSO	11070.080	33562	11057	27	122	2	
HD 11909 .....	HIP 9110	NSO	11438.923	-6173	11430	13	137	4	L
HD 14802 .....	HIP 11072	NSO	11170.808	18824	10863	709	418	7	L
HD 17037 .....	HIP 12764	NSO	11581.755	16915	11452	1295	560	14	L
HD 18445 .....	HIP 13769	NSO	11580.723	49877	11491	1147	222	10	C
HD 21017 .....	HIP 15861	NSO	11779.008	8561	11455	74	371	5	L
HD 25329 .....	HIP 18915	M	11412.131	-25177	11179	361	338	3	
HD 25535 .....	HIP 18824	NSO	10786.825	10205	10576	421	203	2	
HD 28388 .....	HIP 20802	NSO	11170.888	17748	10942	457	498	6	L
HD 29461 .....	HIP 21654	NSO	11581.849	40518	11763	563	116	8	L
HD 29587 .....	HIP 21832	NSO	11073.077	111729	10856	610	786	4	
HD 30339 .....	HIP 22429	NSO	12003.721	12208	11911	211	1538	10	CO
HD 30649 .....	HIP 22596	NSO	11582.778	28904	11391	1545	108	14	L
HD 31412 .....	HIP 22919	NSO	11581.861	47494	11317	1062	144	12	L
HD 32387 .....	HIP 23550	NSO	11072.132	54468	10759	706	1819	3	
HD 32450 .....	HIP 23452	M	11073.049	-11004	10956	233	380	2	
HD 34101 .....	HIP 24419	NSO	11073.046	33664	10950	1942	2543	7	CO
HD 35956 .....	HIP 25662	NSO	11551.891	9942	11346	1822	2457	14	C
HD 39587 .....	HIP 27913	NSO	10068.858	-12171	8846	4580	1294	38	CO
HD 43587 .....	HIP 29860	NSO	11582.848	5776	11160	1638	3361	14	C
HD 50639 .....	HIP 33109	NSO	11552.956	-2947	11412	1169	207	8	L
HD 54563 .....	HIP 34608	NSO	10784.061	-15291	10553	365	8953	4	
HD 64468 .....	HIP 38657	NSO	11581.909	-10624	11267	1541	3991	13	C
HD 65430 .....	HIP 39064	NSO	11581.938	-28709	11214	1846	470	26	CO
HD 68988 .....	HIP 40687	NSO	12064.768	-69520	11919	513	120	13	C
HD 72780 .....	HIP 42112	NSO	11626.698	28059	11693	412	169	10	L
HD 73512 .....	HIP 42418	NSO	11171.030	10737	11199	56	29558	2	
HD 73668 .....	HIP 42488	NSO	11229.858	-21456	11270	775	112	24	L
HD 81133 .....	HIP 45995	NSO	10546.835	11635	10624	400	2456	3	
HD 86680 .....	HIP 49060	NSO	11974.896	7317	11935	91	4728	8	L
HD 89744 .....	HIP 50786	NSO	11698.722	-5401	11675	737	166	45	C
HD 94340 .....	HIP 53217	NSO	10545.893	-15203	10518	84	5126	3	
HD 100167.....	HIP 56257	NSO	11242.931	-27596	11037	411	4649	2	
HD 101206.....	HIP 56829	M	11551.097	40597	11107	945	22398	5	C
HD 101563.....	HIP 57001	NSO	10955.788	-9602	10745	494	656	5	L
HD 102540.....	HIP 57574	NSO	10955.792	-4260	10745	494	4055	5	L
HD 103829.....	HIP 58318	NSO	12101.779	-552	11987	202	128	8	L
HD 106252.....	HIP 59610	NSO	11628.817	15368	11767	1209	114	15	C
HD 111312.....	HIP 62505	NSO	11582.041	623	11186	1119	1094	5	
HD 114762.....	HIP 64426	NSO	9858.733	49576	9723	4069	434	66	C
HD 117126.....	HIP 65708	NSO	11026.672	-7637	10975	195	1685	5	
HD 117176.....	HIP 65721	NSO	9124.792	5036	9853	4928	182	106	C
HD 117635.....	HIP 65982	NSO	10954.918	-51998	10752	492	336	3	
HD 120136.....	HIP 67275	NSO	8779.738	-16542	9558	5097	340	93	C
HD 120690.....	HIP 67620	NSO	10606.790	7159	10535	144	984	2	
HD 122676.....	HIP 68634	NSO	11004.712	-8017	10955	196	1419	3	
HD 122742.....	HIP 68682	NSO	10504.970	-8081	8986	3545	3712	24	CO
HD 129814.....	HIP 72043	NSO	11680.036	6727	11474	1266	101	13	L
HD 131511.....	HIP 72848	NSO	9914.784	-31806	8966	2866	8832	20	CO
HD 131976.....	HIP 73182	M	10181.904	35628	9298	2958	10056	9	C
HD 136118.....	HIP 74948	NSO	11627.902	-3062	11660	1326	136	40	C
HD 136580.....	HIP 75039	NSO	11627.962	-25626	11463	1291	204	19	L
HD 140913.....	HIP 77152	NSO	11304.900	-18679	10474	1511	742	12	CO
HD 142229.....	HIP 77810	NSO	11704.927	-21443	11660	758	486	9	L
HD 142267.....	HIP 77801	NSO	10603.902	35666	10440	328	3931	2	

TABLE 2—*Continued*

Primary Name (1)	Alternate Name (2)	Ref. (NSO/M) (3)	JD (−2440000) (4)	RV (m s <sup>−1</sup> ) (5)	⟨JD⟩ (−2440000) (6)	Δ <i>T</i> (days) (7)	σ <sub>rms</sub> (m s <sup>−1</sup> ) (8)	<i>N</i> (9)	Comment (10)
HD 145206.....	HIP 79195	NSO	11407.673	−36942	11379	53	2180	3	
HD 152311.....	HIP 82621	NSO	10713.733	−21385	10622	166	354	3	
HD 157681.....	HIP 84950	NSO	11811.653	−7723	11449	299	133	6	
HD 158222.....	HIP 85244	NSO	10982.968	−14301	11103	413	2698	3	
HD 160346.....	HIP 86400	NSO	10656.768	15947	9951	1456	3724	7	
HD 161198.....	HIP 86722	NSO	10666.816	23951	10516	391	351	3	
HD 161797.....	HIP 86974	NSO	11372.852	−17004	9872	4324	210	53	L
HD 166435.....	HIP 88945	NSO	11026.782	−14403	11017	23	105	4	
HD 167665.....	HIP 89620	NSO	11702.962	7693	11320	1879	322	16	L
HD 168443.....	HIP 89844	NSO	11071.770	−48636	10976	825	182	37	C
HD 169822.....	HIP 90355	NSO	11793.810	−18274	11824	817	312	22	C
HD 171115.....	HIP 91004	NSO	11780.777	−2291	11425	106	175	5	
HD 173667.....	HIP 92043	NSO	8437.936	23043	9353	5165	124	91	
HD 174457.....	HIP 92418	NSO	11755.929	−25820	11700	755	908	9	CO
HD 175518.....	HIP 92918	NSO	11014.815	−66763	11019	22	1946	6	
HD 183255.....	HIP 95575	M	10666.899	−68922	10606	119	10961	3	
HD 184860.....	HIP 96471	NSO	11793.808	63944	11373	1845	514	21	C
HD 186704.....	HIP 97255	NSO	11411.863	−15117	11383	70	3021	4	L
HD 188376.....	HIP 98066	NSO	10713.746	−39136	10492	430	11891	4	
HD 190406.....	HIP 98819	NSO	11411.872	4757	9477	4364	121	52	L
HD 190771.....	HIP 98921	NSO	11826.657	−25063	11478	1072	136	13	L
HD 195019.....	HIP 100970	NSO	11792.783	−91582	11214	788	188	50	C
HD 197214.....	HIP 102264	NSO	10713.839	−21884	10565	437	4096	4	
HD 199918.....	HIP 103735	NSO	10957.090	52560	10661	591	3443	5	
HD 200565.....	HIP 103983	NSO	11792.788	−2425	11702	793	137	24	L
HD 208527.....	HIP 108296	NSO	10304.870	4154	10102	2550	133	30	
HD 208776.....	HIP 108473	NSO	11440.695	31491	11150	435	601	10	CO
HD 209779.....	HIP 109110	NSO	11751.921	−17310	11543	335	1722	6	L
HD 215578.....	SAO 108160	NSO	11439.882	−16217	11208	1823	1323	21	L
HD 217303.....	HIP 113562	NSO	11782.895	−36049	11439	96	205	7	
HD 219420.....	HIP 114834	NSO	11049.844	−22295	11027	44	2813	5	L
HD 220077.....	HIP 115279	NSO	11707.121	1521	11727	821	132	20	
HD 223084.....	HIP 117258	NSO	11706.125	2164	11310	701	180	33	L
GJ 84.....	HIP 9724	M	11583.710	23335	11419	1294	867	11	CO
GJ 285.....	HIP 37766	M	11629.714	26531	10322	2280	299	7	
GJ 494.....	HIP 63510	M	12127.800	−11228	12004	546	110	15	A
GJ 595.....	HIP 76901	M	11584.166	84921	11886	898	4624	10	CO
GJ 623.....	HIP 80346	M	10181.925	−26284	9208	3222	1238	12	CO
GJ 873.....	HIP 112460	M	11447.748	413	9714	4401	124	17	
GJ 876.....	HIP 113020	M	11072.938	−1591	10514	4016	181	53	C
HIP 35519.....	SAO 115271	NSO	11552.969	11636	11625	803	1529	5	
HIP 52940.....	BD +13 2311B	NSO	11706.829	25212	11574	1137	1310	15	CO
HIP 57450.....	BD +51 1696	NSO	11679.832	64092	11520	810	1211	10	
CD −32 8503B...	...	NSO	11679.866	20940	11264	724	319	5	

NOTE.— Table 2 is also available in machine-readable form in the electronic edition of the *Astrophysical Journal Supplement*.

<sup>a</sup> Stars with σ<sub>rms</sub> ≥ 100 m s<sup>−1</sup>.

35 m s<sup>−1</sup>. The corresponding uncertainty in the mean is 35/√26 = 7 m s<sup>−1</sup>. Thus, the formal difference in zero points is

$$\langle V_{\text{Present}} - V_{\text{Udry}} \rangle = +53 \pm 7 \text{ m s}^{-1}. \quad (1)$$

Thus, there appears to be a statistically significant difference in the zero point of the velocities reported here compared to those of Udry et al. (1999a) of 53 m s<sup>−1</sup>. We do not know the origin of this difference, nor do we know which scale is more “accurate.” Few studies will be affected by such small differences. But future highly precise proper motion measurements and precise orbit calculations may require such accurate velocities, including proper treatment of gravitational redshift and convective blueshift.

However, the difference between the present velocities and those of Udry et al. (1999a) do exhibit a significant *B*–*V* dependence as seen in Figure 4. The slope of the linear trend is  $-182 \pm 24 \text{ m s}^{-1} \text{ per mag}$  with an rms scatter around the fit of 23 m s<sup>−1</sup>. This dependence is similar to the *B*–*V* dependence seen between the CfA and CORAVEL data (Stefanik, Latham, & Torres 1999; Udry et al. 1999a). This color dependence is likely caused by some spectral type mismatch in one or all of the radial-velocity scales. For solar type stars (near G2 V) where our zero point is well set, we are in good agreement with the CORAVEL velocities, with an offset of only 25 m s<sup>−1</sup> as seen in Figure 4.

According to Udry et al. (1999a) the ELODIE measurements ensure temporal stability of better than 15 m s<sup>−1</sup> dur-

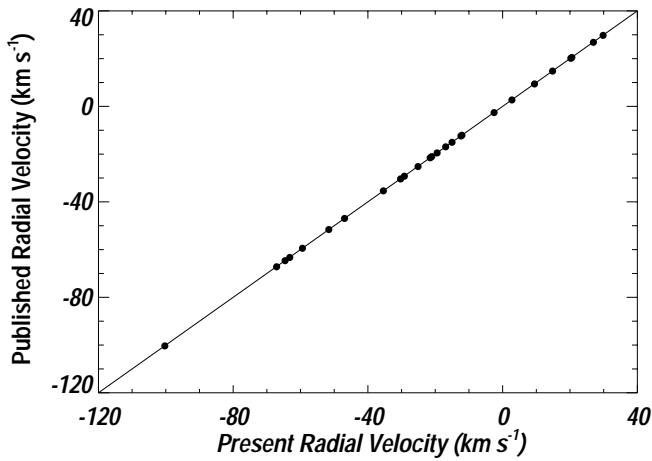


FIG. 2.—Velocities of standard stars vs. velocities measured here, for F, G, and K stars. The standard stars are on the CORAVEL scale (Udry et al. 1999a). The present velocities agree well with the standards, with no visible nonlinear departure of velocity scale.

ing timescales of years for their standard stars. However, their quoted velocities have been rounded off at the  $50 \text{ m s}^{-1}$  level. From our measurements of these stars in common, the temporal variability is less than  $10 \text{ m s}^{-1}$  during  $\sim 5 \text{ yr}$ . Therefore, it is not certain whether the rms scatter of  $35 \text{ m s}^{-1}$  between the two sets of velocities is due to our errors or the rounding of the ELODIE data plus their errors. We conclude that the barycentric velocities reside on the same scale with an offset of  $\sim 50 \text{ m s}^{-1}$ , and a scatter of  $\sim 35 \text{ m s}^{-1}$ .

Comparing our velocities for 29 common stars with those reported by Stefanik et al. (1999), with a correction of  $+136 \text{ m s}^{-1}$  added to their native velocities in Table 1 and 2 (R. P. Stefanik, 2002, private communication), we obtain  $\langle V_{\text{CfA}} - V_{\text{Present}} \rangle = 15 \text{ m s}^{-1}$ , which is only marginally different from zero, with an rms scatter of  $123 \text{ m s}^{-1}$  as seen in Figure 5. The differences exhibit a significant  $B-V$  dependence as seen in Figure 6. The slope of the linear trend is  $+448 \pm 111 \text{ m s}^{-1}$  per mag with an

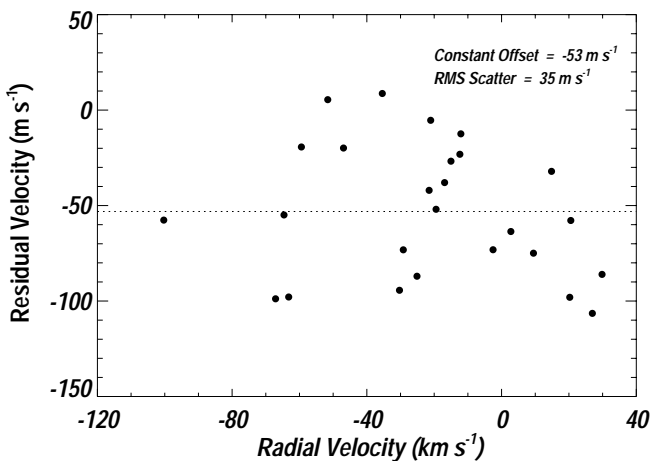


FIG. 3.—Standard-star velocities (Udry et al. 1999a) minus present velocities for all 26 FGK stars in common (as in Fig. 2). The differences reveal that the present velocities are higher than those of Udry et al. by  $53 \text{ m s}^{-1}$  and exhibit an rms scatter of  $35 \text{ m s}^{-1}$ . Thus, the present velocities and those of Udry et al. (1999a) each have internal accuracy better than  $35 \text{ m s}^{-1}$  and differ in zero point by  $\sim 53 \text{ m s}^{-1}$ .

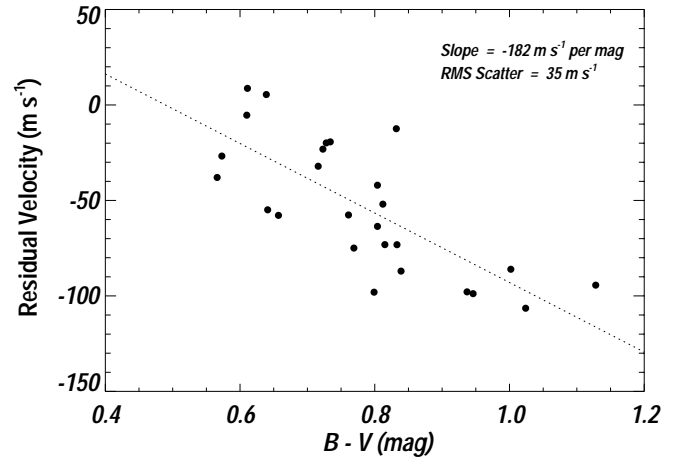


FIG. 4.—Standard-star velocities (Udry et al. 1999a) minus the present velocities as a function of  $B-V$ . A dependence is apparent, suggesting systematic errors in at least one set of velocities. The slope is  $-182 \pm 24 \text{ m s}^{-1}$  per mag. The rms scatter is  $35 \text{ m s}^{-1}$  before fitting and  $23 \text{ m s}^{-1}$  after fitting a line to the data.

rms scatter around the fit of  $109 \text{ m s}^{-1}$ . This color dependence is likely caused by some spectral type mismatch in one or all of the radial-velocity scales. For solar type stars, we are in good agreement with the CfA velocities, with no offset as seen in Figure 6. This is likely due to the CfA velocity zero point being set by observations of minor planets as was also done for the present velocities.

Interestingly, the sign of the slope in Figure 6 is opposite of that in Figure 4 between the CORAVEL and present velocities. Since synthetic spectra were used to derive both the CfA and ELODIE velocities, which were used as the reference system in Udry et al. (1999a), (Stefanik et al. 1999; Baranne et al. 1996; Gullberg 1999) this seems to give credence to the notion that using synthetic spectra does not entirely solve the problem of spectral dependent systematic errors.

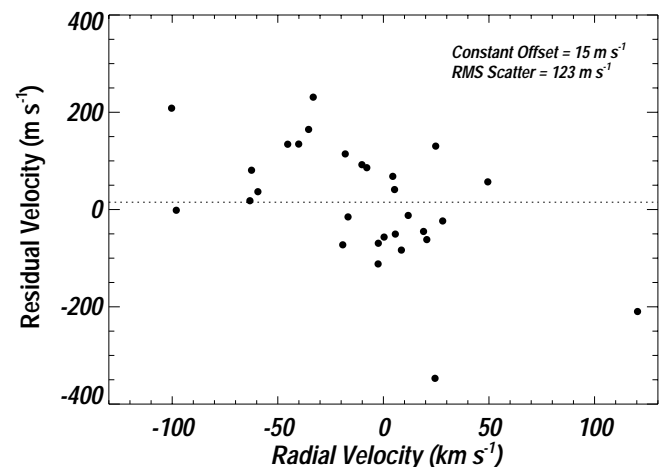


FIG. 5.—Standard-star velocities (Stefanik et al. 1999) minus present velocities for all 29 FGK stars in common. The differences reveal that the present velocities are lower than those of Stefanik et al. by  $15 \text{ m s}^{-1}$  and exhibit an rms scatter of  $123 \text{ m s}^{-1}$ . Thus, the present velocities and those of Stefanik et al. (1999) differ in zero point by  $\sim 15 \text{ m s}^{-1}$ .

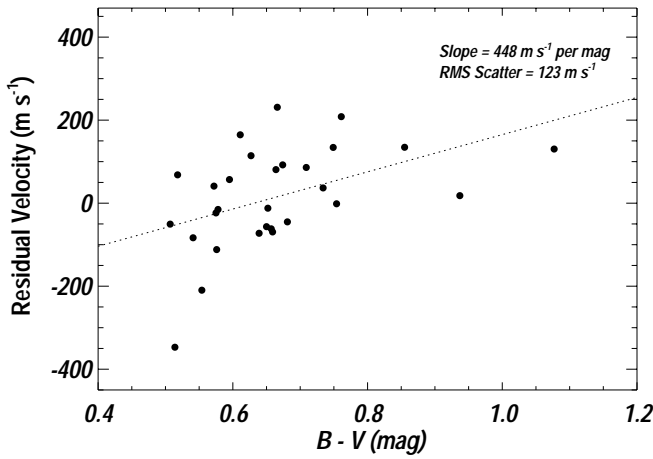


FIG. 6.—Standard-star velocities (Stefanik et al. 1999) minus the present velocities as a function of  $B-V$ . A dependence is apparent, suggesting systematic errors in at least one set of velocities. The slope is  $+448 \pm 111 \text{ m s}^{-1}$  per mag. The rms scatter is  $123 \text{ m s}^{-1}$  before fitting and  $109 \text{ m s}^{-1}$  after fitting a line to the data.

### 6.2. M Stars

The radial-velocity standard stars listed by Udry et al. (1999a) do not include any M dwarfs, and we do not have any M dwarfs in common with Stefanik et al. (1999) or the older CORAVEL standard stars (Udry et al. 1999b). Therefore, we compared our present velocities for M dwarfs to those given in Marcy et al. (1987). The results of this comparison, for 21 stars in common, are shown in Figures 7 and 8 and yield  $\langle V_{\text{MLW}} - V_{\text{Present}} \rangle = -21 \text{ m s}^{-1}$  with an rms scatter of  $164 \text{ m s}^{-1}$ . The offset is obviously very low since the M star reference spectrum was created using the velocities quoted by Marcy et al. (1987). Since the average internal error for the velocities in Marcy et al. (1987) is  $\sim 200 \text{ m s}^{-1}$ , most of the scatter in the differences is due to them. No  $B-V$  dependence is seen in the residuals. It is therefore difficult to ascertain the uncertainty in our present velocities for M dwarfs and similarly difficult to ascertain a zero-point error (whatever that would mean). But a conservative estimate of the errors would be the  $\sim 0.4 \text{ km s}^{-1}$  uncertainty of the

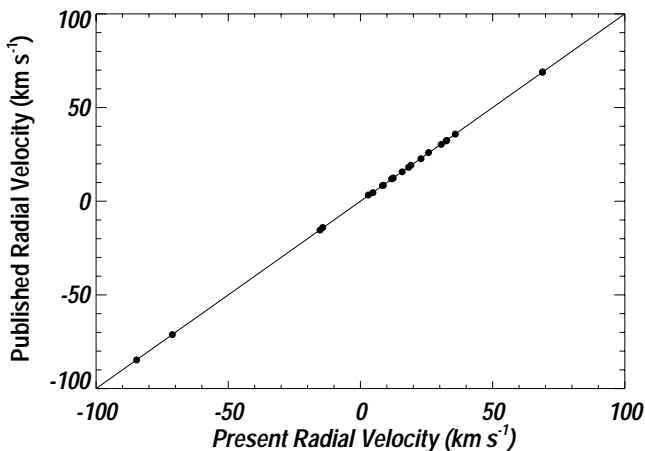


FIG. 7.—Velocities of standard stars (Marcy et al. 1987) vs. present velocities for M dwarfs. The velocities agree well with no apparent nonlinear dependence.

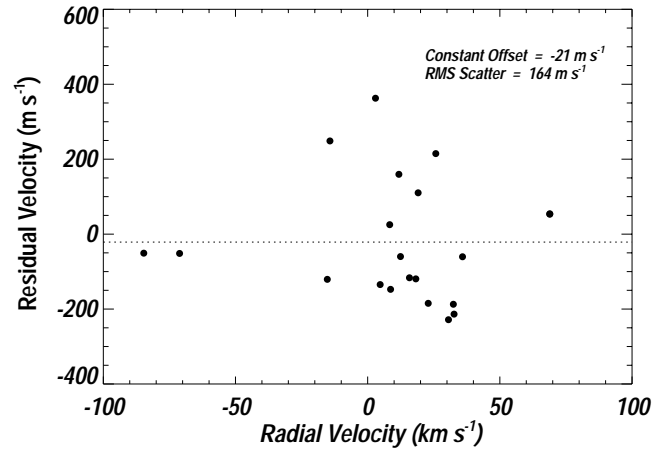


FIG. 8.—Difference between standard stars velocities (Marcy et al. 1987) and present velocities for all 21 M stars in common (as in Fig. 7). There is an rms scatter of  $164 \text{ m s}^{-1}$ , and a constant offset of  $-21 \text{ m s}^{-1}$ , which is not statistically significant. Thus, our velocities for the stars having  $B-V > 1.3$  reside on the velocity scale set by Marcy et al. (1987). No  $B-V$  dependence is seen in the residuals.

Marcy et al. (1987) velocities which were used in setting the velocity zero point.

Since the observed offset ( $21 \text{ m s}^{-1}$ ) for the M dwarfs is within a factor of 2 of the internal scatter of  $\sim 10 \text{ m s}^{-1}$ , we have not applied any correction to the radial velocities for these stars. There is some concern that our two sets of stars, the F, G, and K stars and the M stars, might not be on the same velocity zero point. A comparison between them is difficult due to the significant spectral type mismatch errors.

## 7. UNCERTAINTY ESTIMATES

Due to the several systematic errors affecting radial velocities on the order of  $0.1 \text{ km s}^{-1}$  it is difficult to ascertain the true uncertainties of the velocities reported here. Normally, two different methods are used to estimate uncertainties: (1) Standard deviation of the mean (i.e., the internal rms scatter of points), and (2) comparison with published values. We have done both here. On average the standard deviation of the mean, due to the internal scatter of points, for the velocities in Table 1 is  $\sim 10 \text{ m s}^{-1}$ . We also compared our velocities with the best known published standard star velocities of Udry et al. (1999a). This comparison, as shown in the previous section, gave an rms scatter of the differences of  $35 \text{ m s}^{-1}$ . Therefore, using the traditional methods of estimating uncertainties our velocities are accurate to  $\sim 35 \text{ m s}^{-1}$ .

In this case the traditional methods fail due to the astrophysical sources of errors that affect all spectroscopic measurements of radial velocity. The values of these errors are not known adequately, otherwise we would have corrected for them. It is likely that these systematic errors were also not taken into account by Udry et al. (1999a) or Stefanik et al. (1999). This means that a comparison between their data and ours will not yield the true uncertainty of our velocities or theirs.

What the comparison does show is the precision of velocities within a given spectral type. The velocities of all stars of a given spectral type will have a nearly constant offset from their true kinematic velocities, because the systematic errors are dependent on spectral type. Relative to that constant offset the velocities in that spectral type are very precise. The

comparison with Udry et al. (1999a) shows our precision to be no worse than  $0.035 \text{ km s}^{-1}$  (see Fig. 3).

This high precision within a spectral type can be effectively used to look for moving groups. Moving groups have velocity dispersions of typically  $\sim 0.5 \text{ km s}^{-1}$  such as the Pleiades group (Jones 1970). The present velocities are precise enough within a spectral type to judge whether a star belongs to the moving group or not.

Even though the exact values of the systematic errors are not known we can estimate our true uncertainties. There are three major systematic errors in our velocities, namely, convective blueshift, gravitational redshift, and spectral type mismatch. These errors change systematically with spectral type. Since our velocity zero point was set here using the day sky and the minor planet Vesta, which have well known radial velocities due to solar system dynamics, the systematic errors were forced to zero for solar-type stars. The errors will rise as the spectral type departs from solar type. Because the zero-point calibration was used for all FGK-type stars there will be differential errors due to convective blueshift and gravitational redshift that increase with departure from solar type. Similarly, the spectral type mismatch errors only occur for non-solar-type stars, since the NSO solar spectrum was used for the reference, and is therefore unaffected by the velocity zero-point calibration.

The approximate values of the systematic errors are as follows. According to Dravins (1999) the convective blueshift is approximately  $-1000 \text{ m s}^{-1}$  for F5 V ( $B-V = 0.4$ ),  $-400 \text{ m s}^{-1}$  for G2 V (solar-type,  $B-V = 0.64$ ), and  $-200 \text{ m s}^{-1}$  for K0 V ( $B-V = 0.9$ ). The effective velocity error caused by gravitational redshift can be computed from,  $V_{\text{grav}} = GM/Rc$  (Dravins et al. 1999). We find, with masses and radii given by Allen (2000), that the redshift is  $+680 \text{ m s}^{-1}$  for F5 V,  $+636 \text{ m s}^{-1}$  for G2 V, and  $+590 \text{ m s}^{-1}$  for K0 V. The sum of the two effects shows that the overall systematic error is approximately  $-320 \text{ m s}^{-1}$  for F5 V,  $+236 \text{ m s}^{-1}$  for G2 V, and  $+390 \text{ m s}^{-1}$  for K0 V. Due to our zero-point calibration these errors are here forced to zero for solar-type stars. Therefore, we expect that our velocities are low by  $\sim 556 \text{ m s}^{-1}$  for F5 V stars, true for solar-type stars, and high by  $\sim 154 \text{ m s}^{-1}$  for K0 V stars.

With these estimates of the systematic errors in hand we can compute a correction for the velocities as a function of  $B-V$ . We fit a line to the first two points (F5 V and G2 V) and to the second two points (G2 V and K0 V) to obtain two linear interpolations. The first equation (eq. [2]) is for main-sequence stars earlier than solar type ( $B-V < 0.64$ ), and the second equation (eq. [3]) is for main-sequence stars later than solar type ( $B-V > 0.64$ ), not including M type stars. Equation (3) may be used for stars with  $1.3 > B-V > 0.9$ , but represents an extrapolation of the points given above and should be used with caution. Since most of our main-sequence stars have  $B-V < 1.1$  this should not cause too many problems. These equations do not account for spectral type mismatch errors because we do not know enough about these effects yet for our velocities:

$$\begin{aligned} \text{RV}_{\text{kin}} &= \text{RV}_{\text{spec}} - 2.317 \times (B - V) + 1.483 \text{ km s}^{-1}, \\ B - V &< 0.64; \end{aligned} \quad (2)$$

$$\begin{aligned} \text{RV}_{\text{kin}} &= \text{RV}_{\text{spec}} - 0.642 \times (B - V) + 0.411 \text{ km s}^{-1}, \\ 0.64 &< B - V < 1.3. \end{aligned} \quad (3)$$

These corrections are valid only for main-sequence stars for which the NSO solar spectrum was used as the reference. The velocities for the M type stars, with  $B-V > 1.3$  and for which the M composite spectrum was used as the reference, have a zero-point uncertainty of  $\sim 0.4 \text{ km s}^{-1}$ , and therefore a correction for gravitational redshift or convective blueshift is not warranted at this time. However, we expect the velocities of the M stars to be very precise due to their low rms velocity scatter and their small spectral type range which minimizes the systematic errors. We expect them to also be precise to  $0.03 \text{ km s}^{-1}$ , just as the FGK main-sequence stars. If the “true” radial velocity of only one of them were known then they all could be corrected for their zero-point error and be very accurate.

We expect that the corrections given in equations (2) and (3) account for convective blueshift and gravitational redshift to within  $\sim 0.1 \text{ km s}^{-1}$ . The errors due to spectral type mismatch are likely to be  $\sim 0.1 \text{ km s}^{-1}$  (Griffin et al. 2000). From the errors expressed in equations (2) and (3), an additional  $\sim 0.1 \text{ km s}^{-1}$  for the spectral type mismatch error, along with the distribution of spectral types of our survey stars, the typical uncertainty of the uncorrected radial velocities in Tables 1 and 2 is  $\sim 0.3 \text{ km s}^{-1}$ . For the few subgiants, the errors are somewhat larger, but not easily estimated without models of subphotospheric convection in such stars.

We cannot at this time give a correction for the velocities of our 45 giants. Giants have a gravitational redshift on the order of  $0.1 \text{ km s}^{-1}$ , which is much smaller than that for dwarfs due to the large radius of giants,  $\sim 15 R_{\odot}$  (Allen 2000). The convective blueshift is not known for giants and hinders us from giving a rough velocity correction. Hopefully, more in-depth future studies of the sources of error discussed here, such as recent work by Pourbaix et al. (2002), will allow for more accurate corrections of radial velocities and eventually yield “true” radial velocities. Until that time these corrections may be used for the present velocities.

## 8. FINAL RADIAL VELOCITIES AND DESCRIPTION OF TABLES

The barycentric radial velocities for all 889 stars are reported in Tables 1 and 2. The 782 stars that exhibit an rms velocity scatter less than  $100 \text{ m s}^{-1}$  are reported in Table 1. Primary and alternate star names are given in the first two columns, and the stellar spectrum used as the template (either NSO or M dwarf composite) is listed in column (3). The mean time of the observations is given in column (4) under  $\langle \text{JD} \rangle$  to establish the characteristic epoch for the velocity measurement. The span of observations in days is given in column (5), and the mean barycentric radial velocity of all observations for a star is in column (6). Stars with only one observation were put in Table 1 even though their rms scatter is not defined. They can be distinguished by  $\Delta T = 0$ .

The 107 stars with an rms velocity scatter greater than  $100 \text{ m s}^{-1}$  are reported in Table 2. Primary and alternate star names are given in the first two columns. The stellar template spectrum (either NSO or M dwarf) is given in column (3). The Julian Date (JD) of one specific observation is given in column (4). The barycentric radial velocity of that one observation is given in column (5). The mean date of all observations and span of observations are given in columns

TABLE 3  
ORBITAL PARAMETERS

Star	$P$ (days)	$K$ (km s <sup>-1</sup> )	$e$	$\omega$ (deg)	$T_0$ (-2450000)	$M_1$ ( $M_\odot$ )	$M_{2,\text{min}}$ ( $M_{\text{Jup}}$ )	$a_{\text{min}}$ (AU)	$f(M)$ ( $M_\odot$ )	Other References
HD 4747 .....	6832 (653)	0.65 (0.1)	0.64 (0.06)	257 (5)	453 (473)	0.83	42.3	6.7	0.000087	
HD 7483 .....	701.42 (0.01)	3.02 (0.01)	0.12 (0.003)	313 (0.5)	1791.1 (0.7)	0.92	136	1.6	0.0020	
HD 30339 .....	15.0778 (0.0003)	5.94 (0.01)	0.25 (0.001)	43 (1)	1881.199 (0.0003)	1.10	77.8	0.13	0.00030	
HD 34101 .....	803.51 (0.03)	3.59 (0.01)	0.08 (0.001)	275 (1)	690 (2)	0.87	167	1.7	0.0038	
HD 39587 .....	5136 (12)	1.85 (0.02)	0.45 (0.01)	111 (1)	1463 (17)	0.89	143	5.9	0.0024	
HD 65430 .....	3138 (342)	1.11 (0.2)	0.32 (0.02)	77 (1)	3267 (302)	0.78	67.8	4.0	0.00038	
HD 122742 .....	3617 (7)	6.41 (0.01)	0.48 (0.001)	183 (0.1)	2030 (3)	0.96	545	5.3	0.0670	1, 2, 3, 4, 5
HD 131511 .....	125.396 (0.001)	19.10 (0.01)	0.51 (0.001)	219 (0.1)	203.407 (0.004)	0.78	455	0.52	0.0580	6, 7
HD 140913 .....	147.968 (0.001)	1.94 (0.01)	0.54 (fixed)	18 (1)	1321.42 (0.02)	0.98	43.2	0.55	0.000067	8, 9, 10, 11
HD 174457 .....	840.80 (0.05)	1.25 (0.01)	0.23 (0.01)	139 (1)	2020 (4)	1.19	65.8	1.9	0.00016	
HD 208776 .....	2624 (371)	5.46 (1.3)	0.27 (0.04)	245 (12)	690 (100)	1.24	511	4.2	0.0400	
GJ 84 .....	6818 (2491)	2.18 (0.2)	0.44 (0.08)	238 (10)	1777 (41)	0.39	115	5.6	0.0054	
GJ 595 .....	62.6277 (0.0001)	6.57 (0.01)	0.26 (0.001)	253 (0.1)	1999.50 (0.02)	0.28	60.0	0.22	0.0017	
GJ 623 .....	1366.1 (0.4)	2.08 (0.04)	0.67 (0.01)	251 (1)	1298 (10)	0.31	42.0	1.7	0.00053	12, 13, 14, 15, 16, 17
HIP 52940 .....	1393.5 (0.2)	2.15 (0.01)	0.37 (0.003)	199 (1)	1541 (2)	1.12	126	2.6	0.0011	

REFERENCES.—(1) Duquennoy & Mayor 1991; (2) Martin et al. 1998; (3) Blazit et al. 1987; (4) Kamper 1987; (5) Wagman 1949; (6) Beavers & Salzer 1983; (7) Kamper & Lyons 1981; (8) Halbwachs et al. 2000; (9) Mazeh et al. 1996; (10) Oetiker et al. 2001; (11) Mayor et al. 1997; (12) McCarthy 1986; (13) Barbieri et al. 1996; (14) Henry & McCarthy 1993; (15) Marcy & Moore 1989; (16) McCarthy & Henry 1987; (17) Lippincott & Worth 1978.

(6) and (7). The rms scatter of the velocities of all observations is given in column (8), and the number of observations in column (9). The last column is for comments where stars with companion orbits or linear trends are noted. “L” indicates that velocities vary linearly with time (see Table 4), “CO” indicates that a companion and its orbit were found, “C” indicates that a published companion exists but an orbit is not given here, and “A” indicates that the star is chromospherically active based on the emission reversal seen at the Ca II H and K lines in our spectra.

The orbital parameters for 15 stars with companions are reported in Table 3. The orbital period  $P$ , velocity semiamplitude  $K$ , eccentricity  $e$ , longitude of periastron  $\omega$ , and time of periastron  $T_0$  are given as well as the primary mass  $M_1$ , minimum secondary mass  $M_{2,\min}$ , minimum semimajor axis  $a_{\min}$ , and the mass function,  $f(M)$ . References are also given to other sources which have information on these stars, their companions, and orbital parameters. The data for stars with linear trends are given in Table 4. The slope of the radial velocity curve and the number of observations is given for 30 stars.

## 9. ORBITS OF BINARIES

We found 107 stars in this program that exhibit an rms velocity scatter greater than  $100 \text{ m s}^{-1}$ . We attempted to fit these with a Keplerian orbit. We found 29 stars that yield

TABLE 4  
STARS WITH LINEAR TRENDS

Primary Name	Alternate Name	Slope ( $\text{m s}^{-1} \text{ day}^{-1}$ )	Number of Observations
HD 3770 .....	HIP 3169	0.41 (0.02)	13
HD 3795 .....	HIP 3185	0.363 (0.003)	24
HD 11909 .....	HIP 9110	23.7 (0.8)	4
HD 14802 .....	HIP 11072	-1.73 (0.02)	7
HD 17037 .....	HIP 12764	-1.5 (0.1)	14
HD 21017 .....	HIP 15861	-11.3 (0.3)	5
HD 28388 .....	HIP 20802	-2.7 (0.3)	6
HD 29461 .....	HIP 21654	0.58 (0.02)	9
HD 30649 <sup>a</sup> .....	HIP 22596	0.27 (0.02)	15
HD 31412 .....	HIP 22919	0.414 (0.009)	12
HD 50639 .....	HIP 33109	-0.51 (0.01)	8
HD 72780 .....	HIP 42112	-0.91 (0.03)	10
HD 73668 .....	HIP 42488	-0.69 (0.02)	24
HD 86680 <sup>b</sup> .....	HIP 49060	112 (7)	8
HD 101563 .....	HIP 57001	-3.22 (0.07)	5
HD 102540 .....	HIP 57574	-19.9 (0.5)	5
HD 103829 .....	HIP 58318	-2.28 (0.07)	8
HD 129814 .....	HIP 72043	-0.224 (0.004)	13
HD 136580 .....	HIP 75039	-0.47 (0.02)	18
HD 142229 .....	HIP 77810	-1.47 (0.06)	9
HD 161797 .....	HIP 86974	-0.147 (0.006)	42
HD 167665 .....	HIP 89620	-0.59 (0.02)	16
HD 186704 <sup>b</sup> .....	HIP 97255	-88 (8)	4
HD 190406 .....	HIP 98819	-0.066 (0.001)	58
HD 190771 .....	HIP 98921	0.30 (0.02)	13
HD 200565 .....	HIP 103983	-0.54 (0.01)	24
HD 209779 .....	HIP 109110	-10.7 (0.1)	6
HD 215578 .....	SAO 108160	-2.51 (0.03)	21
HD 219420 .....	HIP 114834	-135.5 (0.5)	5
HD 223084 .....	HIP 117258	-0.85 (0.04)	33

<sup>a</sup> Exhibits some additional positive curvature.

<sup>b</sup> Exhibits some additional negative curvature.

good Keplerian orbital fits to their relative radial velocities. Many of these binaries have been previously published from our velocities and therefore will not be duplicated here. Several papers contain these previously reported single-line spectroscopic binaries, namely Marcy et al. (1999), Butler et al. (2000), Vogt et al. (2002), Fischer et al. (2002), Cumming et al. (1999), and Marcy et al. (2001b).

For 15 stars, our velocities provide unpublished orbital solutions or reveal unknown companions. These orbits are listed in Table 3 which gives the usual orbital parameters for single-line spectroscopic binaries. Plots of the velocities and the associated Keplerian fits are shown in Figures 9–23. The mass for the primary star for each system was estimated from the catalog by Prieto & Lambert (1999) or by using  $B-V$  and Allen (2000). From the orbital parameters and primary masses, we determined the minimum companion masses ( $M_{\min}$ ), mass functions,  $f(M)$ , and minimum semimajor axes,  $a_{\min}$ , which are also listed in Table 3. The values of  $M_{\min}$  range from  $42 M_{\text{Jup}}$  to  $545 M_{\text{Jup}}$ , and therefore the companions are all candidate brown dwarfs or H-burning stellar companions. The uncertainties in the orbital parameters were found by a Monte Carlo technique in which Gaussian velocity noise was added to the best-fit theoretical velocity curve at the times of observation. We ran 50 trials for each case, with orbital parameters being rederived for each trial. The standard deviations of the resulting orbital parameters were taken as the uncertainties. For some stars the Monte Carlo method underestimated the uncertainties in the orbital parameters. For these stars a more conservative estimate of the uncertainties was made by fitting many different Keplerian orbits to the observed relative radial velocities, without any modeled Gaussian noise, and then looking at the scatter of the parameters produced by the best orbital fits.

The stars HD 4747, HD 65430, and GJ 84 have large orbital uncertainties due to incomplete phase coverage. There were insufficient velocity measurements to constrain the orbit of HD 18445 even though it is known to have a companion (Halbwachs et al. 2000). Thus, it is not listed in Table 3. The eccentricity for HD 140913 was fixed to  $e = 0.54$  (Latham et al. 1989) in performing the Keplerian fit, since not enough points were available to constrain the eccentricity. Only the other four parameters

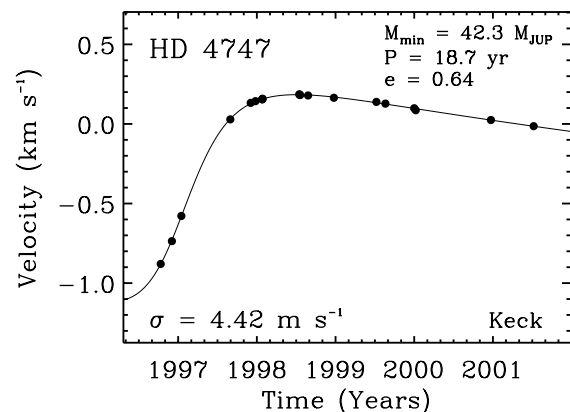


Fig. 9.—Doppler velocities for HD 4747 (G8/K0 V). The solid line is a Keplerian orbital fit with a period of 18.7 yr, a semiamplitude of  $0.65 \text{ km s}^{-1}$ , and an eccentricity of 0.64, yielding a minimum ( $M_{\min}$ ) of  $42.3 M_{\text{Jup}}$  for the companion. The rms of the Keplerian fit is  $4.42 \text{ m s}^{-1}$ .



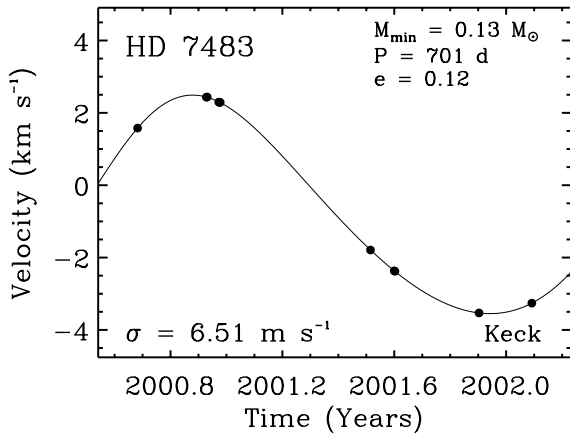


FIG. 10.—Doppler velocities for HD 7483 (G5 V). The solid line is a Keplerian orbital fit with a period of 701 days, a semi-amplitude of  $3.02 \text{ km s}^{-1}$ , and an eccentricity of 0.12, yielding a minimum ( $M_{\min}$ ) of  $0.13 M_{\odot}$  for the companion. The rms of the Keplerian fit is  $6.51 \text{ m s}^{-1}$ .

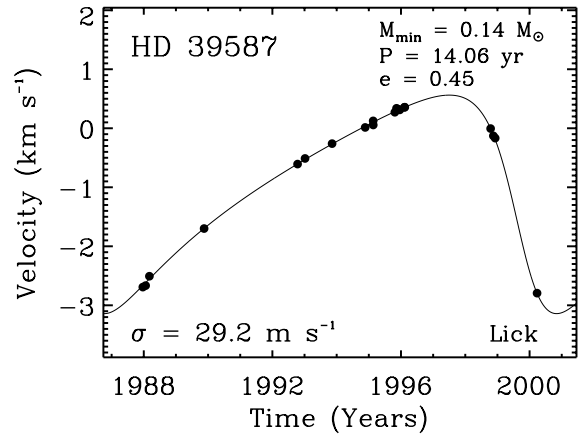


FIG. 13.—Doppler velocities for HD 39587 (G0 V). The solid line is a Keplerian orbital fit with a period of 14.06 yr, a semi-amplitude of  $1.85 \text{ km s}^{-1}$ , and an eccentricity of 0.45, yielding a minimum ( $M_{\min}$ ) of  $0.14 M_{\odot}$  for the companion. The rms of the Keplerian fit is  $29.2 \text{ m s}^{-1}$ .

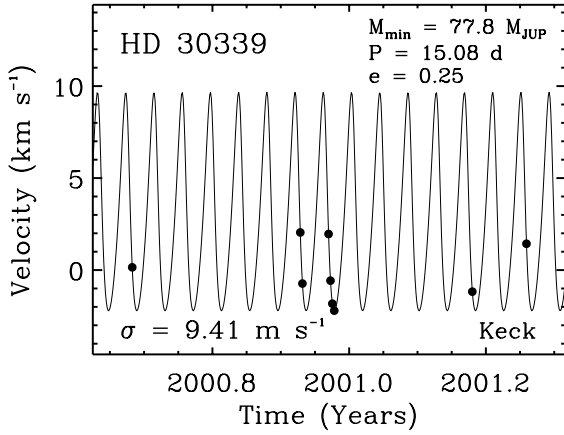


FIG. 11.—Doppler velocities for HD 30339 (F8 V). The solid line is a Keplerian orbital fit with a period of 15.08 days, a semi-amplitude of  $5.94 \text{ km s}^{-1}$ , and an eccentricity of 0.25, yielding a minimum ( $M_{\min}$ ) of  $77.8 M_{\text{JUP}}$  for the companion. The rms of the Keplerian fit is  $9.41 \text{ m s}^{-1}$ .

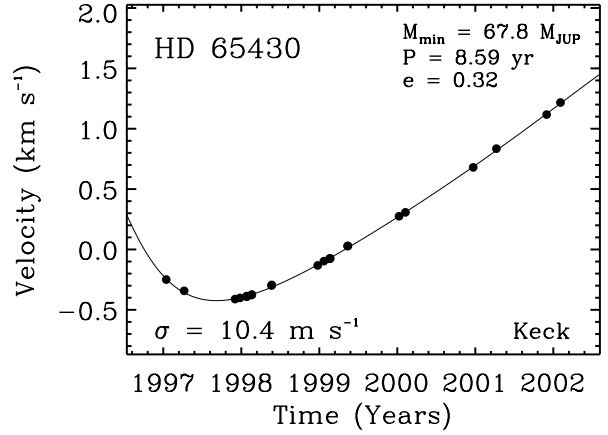


FIG. 14.—Doppler velocities for HD 65430 (K0 V). The solid line is a Keplerian orbital fit with a period of 8.59 yr, a semi-amplitude of  $1.11 \text{ km s}^{-1}$ , and an eccentricity of 0.32, yielding a minimum ( $M_{\min}$ ) of  $67.8 M_{\text{JUP}}$  for the companion. The rms of the Keplerian fit is  $10.4 \text{ m s}^{-1}$ .

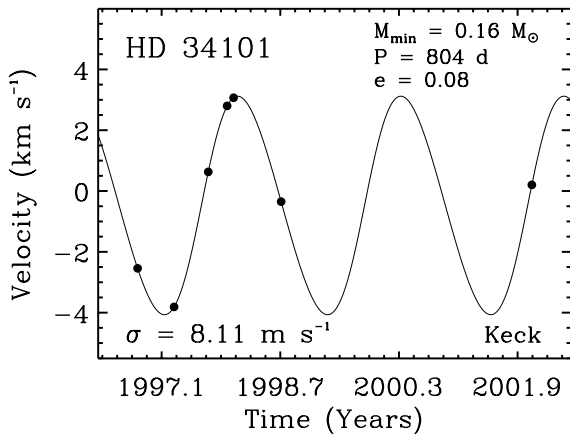


FIG. 12.—Doppler velocities for HD 34101 (G8 V). The solid line is a Keplerian orbital fit with a period of 804 days, a semi-amplitude of  $3.76 \text{ km s}^{-1}$ , and an eccentricity of 0.08, yielding a minimum ( $M_{\min}$ ) of  $0.16 M_{\odot}$  for the companion. The rms of the Keplerian fit is  $8.11 \text{ m s}^{-1}$ .

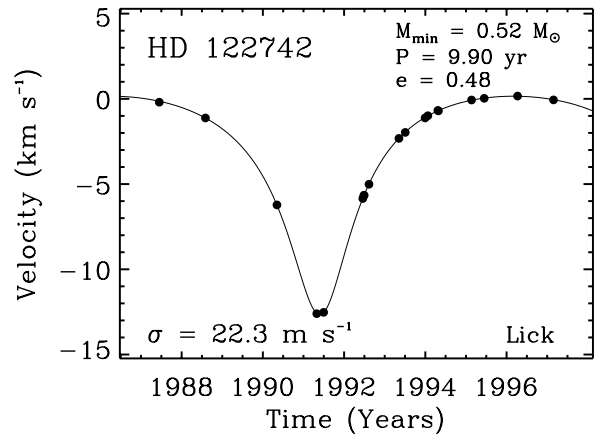


FIG. 15.—Doppler velocities for HD 122742 (G8 V). The solid line is a Keplerian orbital fit with a period of 9.90 yr, a semi-amplitude of  $6.41 \text{ km s}^{-1}$ , and an eccentricity of 0.48, yielding a minimum ( $M_{\min}$ ) of  $0.52 M_{\odot}$  for the companion. The rms of the Keplerian fit is  $22.3 \text{ m s}^{-1}$ .

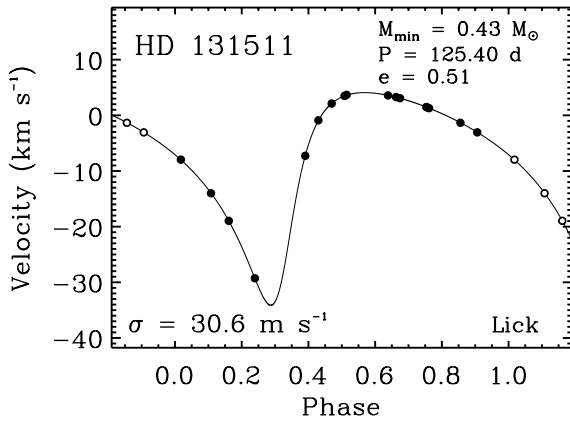


FIG. 16.—Doppler velocities for HD 131511 (K2 V). The solid line is a Keplerian orbital fit with a period of 125.40 days, a semi-amplitude of 19.10  $\text{km s}^{-1}$ , and an eccentricity of 0.51, yielding a minimum ( $M_{\min}$ ) of  $0.43 M_{\odot}$  for the companion. The rms of the Keplerian fit is  $30.6 \text{ m s}^{-1}$ .

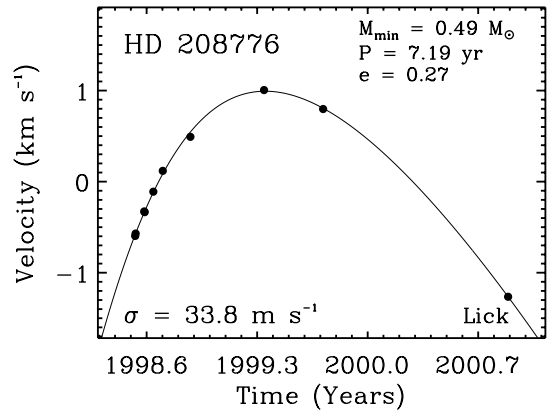


FIG. 19.—Doppler velocities for HD 208776 (G0 V). The solid line is a Keplerian orbital fit with a period of 7.19 yr, a semi-amplitude of  $5.46 \text{ km s}^{-1}$ , and an eccentricity of 0.27, yielding a minimum ( $M_{\min}$ ) of  $0.49 M_{\odot}$  for the companion. The rms of the Keplerian fit is  $33.8 \text{ m s}^{-1}$ .

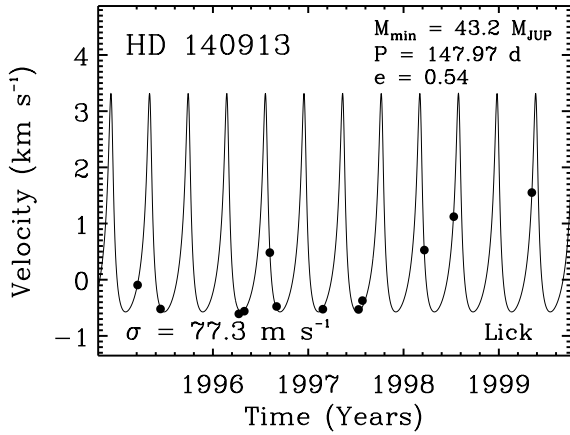


FIG. 17.—Doppler velocities for HD 140913 (G0 V). The solid line is a Keplerian orbital fit with a period of 147.97 days, a semi-amplitude of  $1.94 \text{ km s}^{-1}$ , yielding a minimum ( $M_{\min}$ ) of  $43.2 M_{\text{JUP}}$  for the companion. The eccentricity was fixed to  $e = 0.54$  given by Latham et al. (1989) since not enough points were available to constrain the eccentricity. The rms of the Keplerian fit is  $77.3 \text{ m s}^{-1}$ .

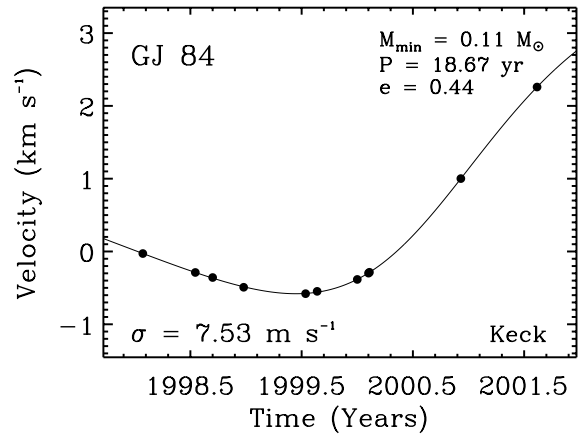


FIG. 20.—Doppler velocities for GJ 84 (M3 V). The solid line is a Keplerian orbital fit with a period of 18.67 yr, a semi-amplitude of  $2.18 \text{ km s}^{-1}$ , and an eccentricity of 0.44, yielding a minimum ( $M_{\min}$ ) of  $0.11 M_{\odot}$  for the companion. The rms of the Keplerian fit is  $7.53 \text{ m s}^{-1}$ .

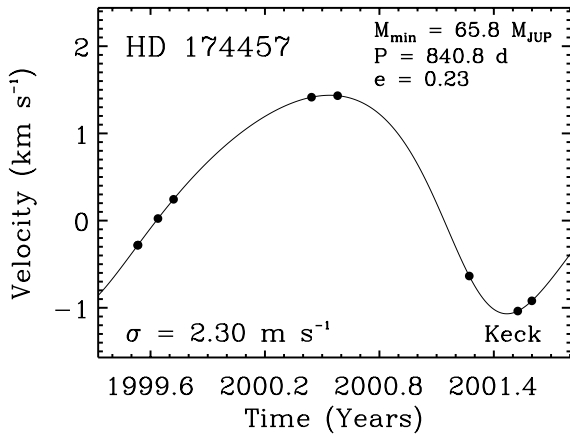


FIG. 18.—Doppler velocities for HD 174457 (F8 V). The solid line is a Keplerian orbital fit with a period of 840.8 days, a semi-amplitude of  $1.25 \text{ km s}^{-1}$ , and an eccentricity of 0.23, yielding a minimum ( $M_{\min}$ ) of  $65.8 M_{\text{JUP}}$  for the companion. The rms of the Keplerian fit is  $2.30 \text{ m s}^{-1}$ .

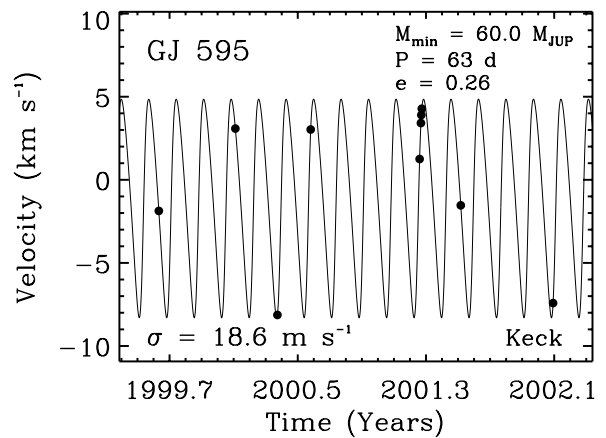


FIG. 21.—Doppler velocities for GJ 595 (M3 V). The solid line is a Keplerian orbital fit with a period of 63 days, a semi-amplitude of  $6.57 \text{ km s}^{-1}$ , and an eccentricity of 0.26, yielding a minimum ( $M_{\min}$ ) of  $60.0 M_{\text{JUP}}$  for the companion. The rms of the Keplerian fit is  $18.6 \text{ m s}^{-1}$ .

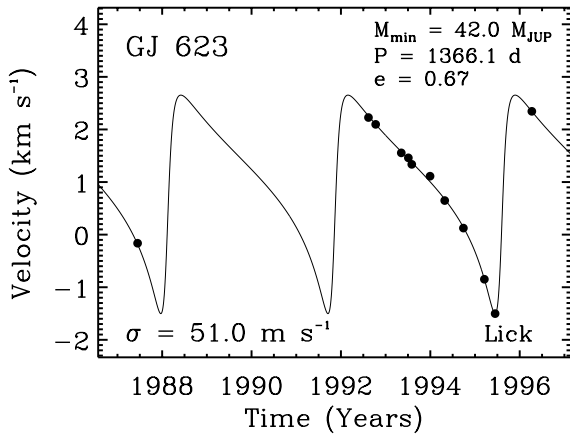


FIG. 22.—Doppler velocities for GJ 623 (M3 V). The solid line is a Keplerian orbital fit with a period of 1366.1 days, a semi-amplitude of  $2.08 \text{ km s}^{-1}$ , and an eccentricity of 0.67, yielding a minimum ( $M_{\min}$ ) of  $42.0 M_{\text{JUP}}$  for the companion. The rms of the Keplerian fit is  $51.0 \text{ m s}^{-1}$ .

were fitted for this star. The Keplerian fit for HD 208776 is particularly poor as insufficient velocities are available to constrain the orbital period to better than a factor of 2. Eleven of the spectroscopic binary stars appear to be newly discovered here: HD 4747, HD 7483, HD 30339, HD 34101, HD 39587, HD 65430, HD 174457, HD 208776, GJ 84, GJ 595, HIP 52940. Velocities are available upon request of G. M. The companions all have  $M_{\min}$  in the substellar range or low-mass stellar range and thus offer interesting targets for studies with adaptive optics or interferometry.

## 10. CONCLUSION

We have provided barycentric radial velocities with an internal precision of  $0.03 \text{ km s}^{-1}$  for 889 stars. The error estimates stem both from the internal errors found from the spectral chunks within each spectrum and from the comparison with accurate velocities on the CORAVEL scale (Udry et al. 1999a). The radial velocities of the F, G, and K dwarfs reside on a velocity zero point defined by the observations of the Sun, using the day sky and Vesta as proxies. Our velocity scale differs by only  $0.053 \text{ km s}^{-1}$  from that of Udry et al. (1999a) and  $0.015 \text{ km s}^{-1}$  from that of Stefanik et al. (1999), thus adding confidence to the zero points of all three sets of velocities. The radial velocities of the M dwarfs reside on the velocity system defined by Marcy et al. (1987) and have not been further corrected, nor is such a correction known to be necessary. These M dwarf velocities are probably accurate to within  $200 \text{ m s}^{-1}$ .

The Doppler shifts reported here have such high accuracy that gravitational redshift and convective blueshift impose comparable (or greater) wavelength shifts. These effects were somewhat removed from our velocity measurements by using the Sun for the velocity zero point. We expect therefore that for G2 V stars the present velocities represent their “true” kinematic velocities within  $0.03 \text{ km s}^{-1}$ . However, for stars departing from solar type the sum of the two astrophysical effects will produce systematic errors dependent on spectral type. From F to K type dwarfs this variation will be as large as  $\sim 0.3 \text{ km s}^{-1}$  and will cause our velocities to be low for F type stars and high for K type stars. Using estimates for these effects we give rough velocity corrections

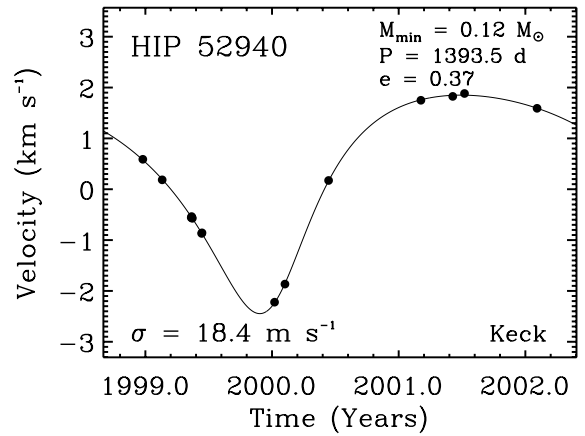


FIG. 23.—Doppler velocities for HIP 52940 (F8 V). The solid line is a Keplerian orbital fit with a period of 1393.5 days, a semi-amplitude of  $2.15 \text{ km s}^{-1}$ , and an eccentricity of 0.37, yielding a minimum ( $M_{\min}$ ) of  $0.12 M_{\odot}$  for the companion. The rms of the Keplerian fit is  $18.4 \text{ m s}^{-1}$ .

in equations (2) and (3). We presume that these corrections bring the velocities within  $\sim 0.15 \text{ km s}^{-1}$  of their “true” kinematic values.

These precise radial velocities can be used to complement future highly precise proper motion measurement, such as those projected to be obtained by the GAIA mission of the ESA. The radial velocities and proper motions will give the three components of space motion of stars. These precise space motions may be useful for discerning the membership of moving groups, since young moving groups have velocity dispersions of  $\sim 0.5 \text{ km s}^{-1}$  (Jones 1970).

The 782 stars listed in Table 1 exhibited a velocity scatter of less than  $100 \text{ m s}^{-1}$  during 4 years. These stars apparently exhibit relatively stable velocities on timescales of a decade and represent candidates for radial velocity standard stars. However, their integrity as velocity standard stars requires future observations to verify their stability. We expect that some of these 782 “stable” stars may reveal slow drifts in radial velocity on timescales longer than 10 yr.

The accuracy of the present velocities offers an opportunity to detect such slow drifts by future measurements made with comparable accuracy. Such velocity variations may prove useful in identifying unseen companions at large orbital distances, i.e., over 10 AU. We found that 107 stars exhibited velocity variations of over  $100 \text{ m s}^{-1}$  (rms). For these stars, we have provided the rms velocity, and also either an orbital solution or a description of the linear trends. We intend these measurements to provide dynamical constraints on the nature of the companions.

We acknowledge support by NSF grant AST-9988358 (to S. S. V.), NSF grant AST-9988087 and travel support from the Carnegie Institution of Washington (to R. P. B.), NASA grant NAG5-8299 and NSF grant AST95-20443 (to G. W. M.), and by Sun Microsystems. We thank the NASA and UC Telescope assignment committees for allocations of Keck telescope time, and we thank the University of California for generous allocations of telescope time at Lick Observatory. This research has made use of the SIMBAD database, operated at CDS, Strasbourg, France. We would like to thank A. Reines, C. McCarthy, E.J. Anderson, and S. White for all of their help and inspiration.

## REFERENCES

- Allen, C. W. 2000, *Astrophysical Quantities* (4th ed.; New York: AIP Press)
- Allende Prieto, C., García López, R. J., & Trujillo Bueno, J. 1997, *ApJ*, 483, 941
- Baranne, A. 1999, in *IAU Colloq. 170, Precise Stellar Radial Velocities*, ed. J. B. Hearnshaw & C. D. Scarfe (Dordrecht: Kluwer), 1
- Baranne, A., et al. 1996, *A&AS*, 119, 337
- Barbieri, C., Demarchi, G., Nota, A., Corrain, G., Hack, W., Ragazzoni, R., & Macchetto, D. 1996, *A&A*, 315, 418
- Beavers, W. I., & Salzer, J. J. 1983, *PASP*, 95, 79
- Binney, J., & Merrifield, M. 1998, in *Galactic Astronomy* (Princeton: Princeton Univ. Press), 38
- Blazit, A., Bonneau, D., & Foy, R. 1987, *A&AS*, 71, 57
- Bouchy, F., Pepe, F., & Queloz, D. 2001, *A&A*, 374, 733
- Butler, R. P., Marcy, G. W., Williams, E., McCarthy, C., Dosanji, P., & Vogt, S. S. 1996, *PASP*, 108, 500
- Butler, R. P., Vogt, S. S., Marcy, G. W., Fischer, D. A., Henry, G. W., & Apps, K. 2000, *ApJ*, 545, 504
- Carroll, B. W., & Ostlie, D. A. 1996, *An Introduction to Modern Astrophysics* (New York: Addison-Wesley), 14
- Cumming, A., Marcy, G. W., & Butler, R. P. 1999, *ApJ*, 526, 890
- Dravins, D. 1999, in *IAU Colloq. 170, Precise Stellar Radial Velocities*, ed. J. B. Hearnshaw & C. D. Scarfe (Dordrecht: Kluwer), 268
- Dravins, D., Gullberg, D., Lindegren, L., & Madsen, S. 1999, in *IAU Colloq. 170, Precise Stellar Radial Velocities*, ed. J. B. Hearnshaw & C. D. Scarfe (Dordrecht: Kluwer), 41
- Duquenois, A., & Mayor, M. 1991, *A&A*, 248, 485
- Fischer, D. A., et al. 2002, *PASP*, in press
- Gray, D. F. 1999, in *IAU Colloq. 170, Precise Stellar Radial Velocities*, ed. J. B. Hearnshaw & C. D. Scarfe (Dordrecht: Kluwer), 243
- Griffin, R. E. M., David, M., & Verschueren, W. 2000, *A&AS*, 147, 299
- Gullberg, D. 1999, *IAU Colloq. 170, Precise Stellar Radial Velocities*, ed. J. B. Hearnshaw & C. D. Scarfe (Dordrecht: Kluwer), 58
- Halbwachs, J. L., Arenou, F., Mayor, M., Udry, S., & Queloz, D. 2000, *A&A*, 355, 581
- Henry, T. J., & McCarthy, D. W., Jr. 1993, *AJ*, 106, 773
- Jones, B. F. 1970, *AJ*, 75, 563
- Kamper, K. W. 1987, *AJ*, 93, 683
- Kamper, K. W., & Lyons, R. W. 1981, *JRASC*, 75, 56
- Kurucz, R. L., Furenlid, I., & Brault, J. 1984, *Flux Atlas from 296 to 1300 nm* (Sunspot: National Solar Obs.)
- Latham, D. W., Mazeh, T., Stefanik, R. P., Mayor, M., & Burki, G. 1989, *Nature*, 339, 38
- Lindegren, L., Dravins, D., & Madsen, S. 1999, in *IAU Colloq. 170, Precise Stellar Radial Velocities*, ed. J. B. Hearnshaw & C. D. Scarfe (Dordrecht: Kluwer), 73
- Lippincott, S. L., & Worth, M. D. 1978, *PASP*, 90, 330
- Marcy, G. W., & Butler, R. P. 1992, *PASP*, 104, 270
- Marcy, G. W., Butler, R. P., Fischer, D., Vogt, S. S., Lissauer, J. J., & Rivera, E. J. 2001b, *ApJ*, 556, 296
- Marcy, G. W., Butler, R. P., Vogt, S. S., Fischer, D., & Liu, M. C. 1999, *ApJ*, 520, 239
- Marcy, G. W., Cochran, W. D., & Mayor, M. 2000, in *Protostars and Planets IV*, ed. V. Mannings, A. P. Boss & S. S. Russell (Tucson: Univ. Arizona Press), 1285
- Marcy, G. W., Lindsay, V., & Wilson, K. 1987, *PASP*, 99, 490
- Marcy, G. W., & Moore, D. 1989, *ApJ*, 341, 961
- Martin, C., Mignard, F., Hartkopf, W. I., & McAlister, H. A. 1998, *A&AS*, 133, 149
- Mayor, M., Queloz, D., Udry, S., & Halbwachs, J. L. 1997, in *IAU Colloq. 161, Astronomical and Biochemical Origins and the Search for Life in the Universe*, ed. C. S. Cosmovici, S. Bowyer, & D. Werthimer (Bologna: Editrice Compositori), 313
- Mazeh, T., Latham, D. W., & Stefanik, R. P. 1996, *ApJ*, 466, 415
- McCarthy, C. 1995, M.S. thesis, San Francisco State Univ.
- McCarthy, D. W., Jr. 1986, in *Astrophysics of Brown Dwarfs*, ed. M. C. Kafatos, R. S. Harrington, & S. P. Maran (Cambridge: Cambridge Univ. Press), 9
- McCarthy, D. W., Jr., & Henry, T. J. 1987, *ApJ*, 319, L93
- Misner, C. W., Thorne, K. S., & Wheeler, J. A. 1973, *Gravitation* (San Francisco: Freeman)
- Oetiker, B., Duric, N., McGraw, J. T., & McGrath, M. A. 2001, *PASP*, 113, 703
- Pepe, F., et al. 2000, *Proc. SPIE*, 4008, 582
- Perryman et al. 1996, *A&A*, 310, L21
- Pourbaix, D., et al. 2002, *A&A*, 386, 280
- Prieto, C. A., & Lambert, D. L. 1999, *A&A*, 352, 555
- Saar, S. H., & Fischer, D. 2000, *ApJ*, 534, L105
- Stefanik, R. P., Latham, D. W., & Torres, G. 1999, in *IAU Colloq. 170, Precise Stellar Radial Velocities*, ed. J. B. Hearnshaw & C. D. Scarfe (Dordrecht: Kluwer), 354
- Udry, S., Mayor, M., & Queloz, D. 1999a, in *IAU Colloq. 170, Precise Stellar Radial Velocities*, ed. J. B. Hearnshaw & C. D. Scarfe (Dordrecht: Kluwer), 367
- Udry, S., et al. 1999b, in *IAU Colloq. 170, Precise Stellar Radial Velocities*, ed. J. B. Hearnshaw & C. D. Scarfe (Dordrecht: Kluwer), 383
- Valenti, J. A., Butler, R. P., & Marcy, G. W. 1995, *PASP*, 107, 966
- Vogt, S. S. 1987, *PASP*, 99, 1214
- Vogt, S. S., et al. 1994, *Proc. Soc. Photo-Opt. Instr. Eng.*, 2198, 362
- Vogt, S. S., Butler, R. P., Marcy, G. W., Fischer, D. A., Pourbaix, D., Apps, K., & Laughlin, G. 2002, *ApJ*, in press
- Vogt, S. S., Marcy, G. W., Butler, R. P., & Apps, K. 2000, *ApJ*, 536, 902
- Wagman, N. E. 1949, *AJ*, 54, 138